TRAJECTORY TRACKING CONTROL OF QUADROTOR UNMANNED AIRIAL VEHICLE USING SLIDING MODE - FUZZY PROPORTIONAL INTEGRAL DERIVATIVE CONTROLLER

BY

BIRUK TADESSE NADEW

A Thesis Submitted as a Partial Fulfillment for the Degree of Master of Science in Electrical and Computer Engineering (Control and Instrumentation Engineering)

to

DEPARTMENT OF ELECTRICAL AND COMPUTER ENGINEERING

ADDIS ABABA SCIENCE AND TECHNOLOGY UNIVERSITY

OCTOBER 2019

Certificate

This is to certify that the thesis prepared by **Mr. Biruk Tadesse Nadew** entitled "**Trajectory Tracking Control of Quadrotor Unmanned Aerial Vehicle Using Sliding Mode-Fuzzy PID Controller"** and submitted in fulfillment of the requirements for the Degree of Master of Science complies with the regulations of the University and meets the accepted standards with respect to originality and quality.

Singed by Examining Board:

External Examiner: Signature, Date:

_____ _____ _____

Internal Examiner: Signature,
Date:

_____ _____ _____

Chairperson: Signature,
Date:

_____ _____ _____

DGC Chairperson: Signature, Date:

_____ _____ _____

Collage Dean/Associate Dean for GP Signature, Date:

_____ _____ _____

Declaration

I hereby declare that this thesis entitled "**Trajectory Tracking Control of Quadrotor Unmanned Aerial Vehicle Using Sliding Mode-Fuzzy PID Controller"** was composed by myself, with the guidance of my advisor, that the work contained herein is my own except where explicitly stated otherwise in the text, and that this work has not been submitted, in whole or in part, for any other degree or processional qualification.

Author: Signature, Date:

Biruk Tadesse _____ _____

Witnessed by:

Name of student advisor; Signature, Date:

Asrat Mulatu (PhD.) _____ _____

Name of student co-advisor Signature, Date:

Beza Nekatibeb (PhD. candidate) _____ _____

Abstract

In this thesis, trajectory tracking control of quadrotor Unmanned Aerial Vehicle (UAV) is done by controlling attitude and position of the quadrotor using Sliding Mode Controller (SMC) and fuzzy Proportional, Integrator and Derivative (PID) controller, simultaneously.

Quadrotor UAV have been an increasingly popular research topic in recent years due to their low cost, maneuverability, simplicity of structure, ability to hover, vertical take-off and landing (VTOL) capacity and ability to perform variety of tasks. Here two type of controllers were used to track reference trajectories with improved performance. SMC is used for position and altitude (translational dynamics), whereas fuzzy PID controller is used for attitude and heading (rotational dynamics). Dynamic modeling of the quadrotor was derived using Newton-Euler formalization including aerodynamic effects. The proposed SMC and fuzzy PID controller strategies were designed for the non-linear quadrotor dynamics. The controller robustness are tested by adding external random disturbance on the out state. The control performance of SMC alone and mixed sliding mode-fuzzy PID controller are compared. Finally, the behavior of the quadrotor under the proposed control system was validated by using MATLAB/Simulink. The simulation results showed that the performance of the proposed control scheme have better trajectory performance and good disturbance rejection ability.

Keywords: *Quadrotor, UAV, Dynamic modeling, SMC, Fuzzy PID control*

Acknowledgments

First of all I would like to thank Addis Ababa science and Technology University as well as Electrical and Mechanical Engineering College allowing me to join this Master's program in Control and Instrumentation Engineering.

I feel privileged and honored to express my sincere gratitude to my advisor Dr. Asrat Mulatu for his kind help, guidance, suggestions and support throughout this research work. I would also like to express my endless gratitude to my co-advisor Mr. Beza Nekatibeb for his guidance and support in completing this thesis.

I would like to express gratitude to Mr. Mulugeta Debebe for who support and gave important reference for this thesis.

I also want to thank my previous advisor Dr. Gopikrishna Pasam who was guided and supported me during proposing and stating phase of this thesis.

I am especially grateful to all the administrative and teaching staff of Electrical and Computer Engineering Department of the college for their unreserved help and cooperation throughout the way.

Biruk Tadesse

Table of Contents

List of Abbreviation and Acronyms

CCW	Counter Clock Wise
CW	Clock Wise
FPID	Fuzzy Proportional, Integrator and Derivative
ISE	Integral Square Error
IAE	Integral Absolute Error
ITSE	Integral Time Square Error
ITAE	Integral Time Absolute Error
LQR	Linear Quadratic Regulator
MIMO	Multiple Input Multiple Output
PID	Proportional, Integrator and Derivative
RPM	Revolution per Minute
SM	Sliding Mode
SMC	Sliding Mode Control
UAV	Unmanned Aerial Vehicle
VTOL	Vertical Take Off and Landing
VSC	Variable Structure Control
b	Thrust constant
d	Drag factor of the rotating propeller
g	Acceleration due to gravity
Ixx	Moment of inertia in roll
Iyy	Moment of inertia in pitch
Izz	Moment of inertia in yaw
J_r	Moment of inertia of rotor
R	Direction cosine matrix
x	Longitudinal coordinate in Earth-fixed frame
y	Lateral coordinate in Earth-fixed frame
z	Vertical coordinate in Earth-fixed frame
Φ	Roll angle of the axis (Euler angles) in (radian)
Θ	Pitch angle of the axis (Euler angles) in (radian)
Ψ	Yaw angle of the axis (Euler angles) in (radian)

List of Tables

List of Figures

Chapter One

Introduction

1.1. Background

Quadrotor Unmanned Aerial Vehicle (UAV) have been an increasingly popular research topic in recent years, because of their low cost, maneuverability, simplicity of structure, ability to hover, vertical take-off and landing (VTOL) capacity and ability to done variety of tasks in control and aerospace engineering. This research is motivated by their numerous applications such as inspection, surveillance, law enforcement, videography, rescue and search and many others. Moreover, this field of study involves many engineering challenges in the areas of control, electrical and mechanical engineering [1].

Starting from World War I up to half of 19th century, UAVs were used only for aviation academy, which means they are designed and built for only military purposes. But here in the 21st century, technology became a point of sophistication that UAV is being given attention for other areas of aviation [2].

Emerging aerospace industry has a niche in performing dangerous and critical missions. It also has been widely used in the military department over the last decade and the success of these military application is increasingly driving efforts to establish unmanned aerial in non-military roles in technologically advanced countries. Whereas, in developing country the use of this UAV or drone is very low. However, the demand of automated systems is constantly increased while the technology is limited basically [3].

The trend in UAV usage is not for a limited purpose but also for multiple purposes by modifying some parts, like it's possible to make security system to aerial camera and videography. While the share of UAV for military purposes decreased, the share for other technology transfer increased day to day. The flight of UAVs may be controlled either by fully autonomously by on-board computers or a given degree of remote control from an operator, located on the ground or in another vehicle [2] [3].

To be able have a UAV system that can fly autonomously doing an action, simplifies human power for contribution, increasing its ability exponentially. Quadrotors is a type of small UAV's in which they get their lift force from the four rotors or motors. It has

six degree of freedom in which three of them are rotational and the remaining are translational. This, in turn, helps in its maneuverability and controllability of the vehicle in space [3] [4].

From the rotorcraft, quadrotor helicopters are usually afford a larger payload than conventional helicopters, since it has four rotors. Moreover, min-quadrotor helicopters possess a great maneuverability and they are simpler to manufacture. This is why quadrotor helicopter have attracted much attention in UAV research and history [2] [4]. The quadrotor also possesses more advantage compared to standard helicopters in terms of small size, efficiency, and safety. Quadrotor is an unmanned aerial, Vertical Take-Off-Landing (VTOL) vehicle that is classified among aerial vehicles with rotary wings. This aerial vehicle has four rotors whose propulsion thrust force and torque is generated by the transmission of power to blades or propellers of the quadrotor and controlled and stabilized by motor rpm or thrust force and torque. Quadrotor is a vehicle with six degrees of freedom, which can be achieved using four actuators, so it can be considered as an under-actuated system [4].

1.2. Statement of the Problem

The accepted nonlinear dynamic model of quadrotor is based on thrust and torque model with constant thrust and torque coefficients derived from static thrust tests. Such a model is no longer valid when the vehicle undertakes dynamic maneuvers that involve significant displacement and velocities [4]-[8]. And, the other problem is that most research works neglect the aerodynamic effects, gyroscopic moment which occurs because of propellers and quadrotor body [5][6]. Which resulted in lowering the performance of trajectory tracking control.

This research addresses the above problems by proposing a thrust model that incorporates the induced momentum effects associated with the rotor and body of quadrotor. And also the air disturbance and aerodynamic drag force and torque are considered in the model. The tracking performance is improved using sliding mode - fuzzy PID controllers. Both sliding mode and Fuzzy PID controller have fast response time, precise tracking, and robustness against disturbances and unpredicted inaccuracies which are existing in a system like UAVs [9][10].

1.3. Objective

1.3.1. General Objective

The general objective of this research work is modeling quadrotor UAV and design sliding mode and fuzzy PID controller for improve trajectory tracking performance.

1.3.2. Specific Objectives

- Derive the nonlinear mathematical model of quadrotor dynamics
- Design nonlinear SMC and fuzzy PID controller for the quadrotor model
- Interface the controller with the nonlinear quadrotor dynamics model on MATLAB/Simulink and build up the system
- Simulate the system and make a thorough performance analysis

1.4. Scope and Limitation

The scope of this research work covers from deriving the nonlinear mathematical model of quadrotor dynamic's up to the simulation of the final system using MATLAB/Simulink software. Its limitation is not to build a prototype for further analysis and study purposes which is due to lack of laboratory setup, equipment and related materials.

1.5. Methodology

In order to meet the specified objectives of this thesis, the first thing to be conducted was literature survey, which means to review what have been done before quadrotor or quadcopter modeling and controlling trajectory tracking techniques. Then follows driving the mathematical model of the quadrotor including the aerodynamic effects and rotor dynamic effects by using both the Newton-Euler formalization. Next sliding mode-fuzzy PID controller was designed and interfaced as shown Fig. 1.5. The model will be implemented and simulated by MATLAB/Simulink.

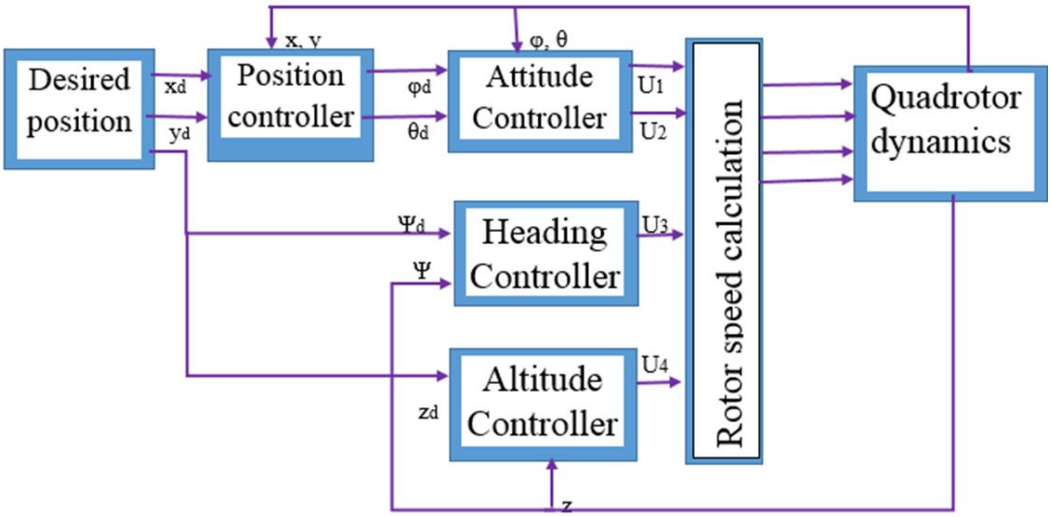

Fig. 1.1: General Quadrotor control scheme block diagram [7]

1.6. Thesis Outline

The rest of this thesis is organized as follows:

Chapter two studies about the previous researchers work and review their merit and demerit. Chapter three deals on how to obtain the nonlinear dynamic modelling of quadrotor or quad-copter and its verification using Matlab/Simulink. And also it studies about the controller strategies of the nonlinear dynamic model of quadrotor that means SMC and fuzzy PID controller. Chapter four provides simulation results and detailed analysis of the proposed system. In the last chapter five concludes and recommends future research directions.

Chapter Two

Literature Review

2.1. Review of literature and Theoretical Background of Quadrotor

Quadrotor controller design and its modeling is a well-known field of research and is used in many civil and military applications, security purposes and in film making for aerial camera and videography. Different literatures have approached the research of quadcopter's control design and modeling in different ways, some of them are discussed as follows.

Quadrotor control needs an accurate model to its dynamic system. The first dynamic model of quadrotor was obtained by Lagrangian method. It was partial differential equation for quadcopter system dynamics, which had been derived from Lagrangian model of quadrotor [3] [4].

The very first experiment practically attempted was to take it off with a rotorcraft were mostly done with multirotor. In 1907, as described in Jacques and Louis Breguet, French brothers built and tested Gyroplane No 1- which is a typical model of a quadcopter. They managed take it-off, although the design controller system found to be a very unstable and hence impractical [4].

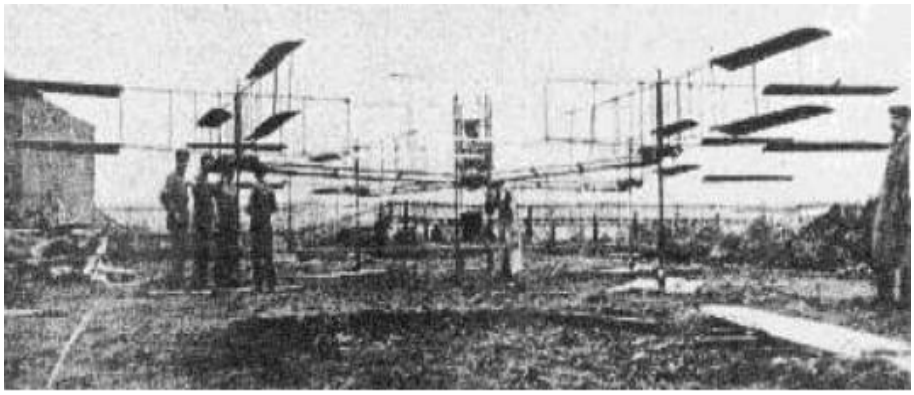

Fig. 2.1: The Breguet-Richet Gyroplane No.1-quadrotor of 1907 [4]

Etienne Oehmichen was the first researcher and scientist who tested with rotorcraft designs in 1920. He demonstrate six different designs, among those the second one was a multi-copter which had eight propellers and four rotors, all controlled by a single engine. It used two-bladed rotors at the ends of the four arms with a steel-tube frame. The angle of these propellers could be varied by warping. Five of the propellers, spinning in the horizontal surface plane, stabilized the machine laterally. Another

propeller was mounted at the nose for steering. The remaining propellers were for forward propulsion [4].

In 1924, it achieved the first-ever Federation Areonautique International (FAI) distance record for helicopters of 360 m. Later, it completed the first 1 kilometer closed-circuit flight by a rotorcraft [1], [4].

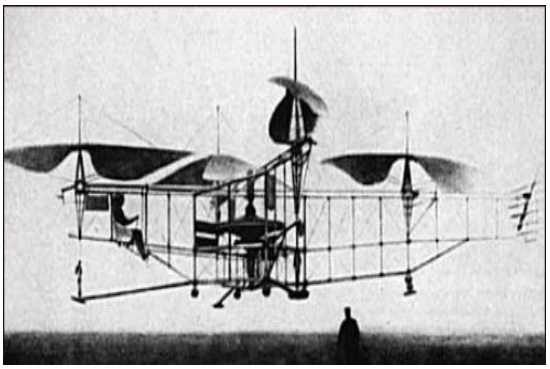

Fig. 2.2: Oehmichen quadrotor No. 2, 1924 [4]

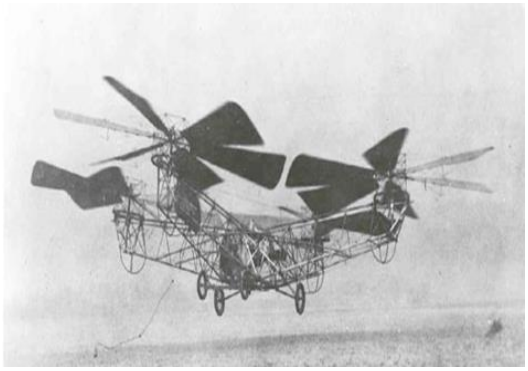

Fig. 2.3: Bothezat quadrotor [4]

After Oehmichen, G. de Bothezat and I. Jerome modified this aircraft with six bladed rotors at the end of an X-shaped configuration. A pair of small propellers with variable pitch were used for thrust and yaw control [4].

Convertawings quadrotor model was proposed to be the prototype for a line of much larger military and civilian quadrotor helicopters. The design prospect uses two engines driving four rotors with wings added for additional lift in forward flight. The control system was obtained by varying the thrust between rotors, no tail rotor was needed. Flown successfully for many times around the mid-1950s, this helicopter proved to be the right quadrotor model design and it was also the first quadrotor helicopter to show successful forward flight. However, due to the lack of materials for commercial or military versions however, the project was terminated [1]-[4].

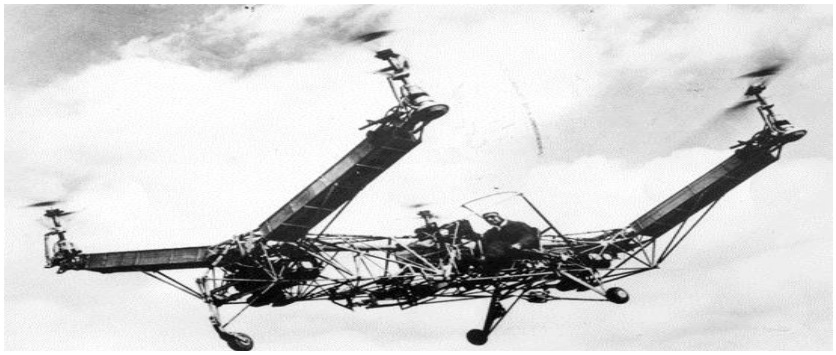

Fig. 2.4: Convertawings quadrotor model 1956 [4]

When it comes to the recent UAV research paper many researcher works on this area. In [5] [6], have demonstrated that it is possible to control the quadrotor UAV using linear control techniques by linearizing the dynamics around an operating point, usually chosen to be the hover. In this case during linearization many unmodeled dynamics was ignored and left from the system which leads to lack of controller performance. However, a wider flight envelope and an excellence performance can be accomplished by using nonlinear control techniques. That considers a more general form of the dynamics of the vehicle in all flight zones. Within these nonlinear control methods, backstepping [7] [8], sliding mode controller [8] [9], and feedback linearization [10] [11], have been demonstrated to be effective for quadrotor control. Even though, most of those study were investigated without considering aerodynamic drag force and torque, gyroscopic torque and unknown external disturbance.

In [12], A. Das *et al*. suggested that dynamic inversion with zero-dynamic stabilization and a feedback linearization structure that divided the quadrotor dynamics into an outer loop containing the position dynamics and an inner loop containing the attitude and altitude of the vehicle. Feedback linearization allows to obtaining a linear model of quadrotor by dynamic inversion linearization method. These control structures show significant promise and is investigated in this work along with linear methods such as LQR (linear quadratic regulator). All the control techniques suggested above require complete knowledge of the system model and the model parameters, but the errors in the identified values of the parameters can lead to important deterioration of the controller performance. Furthermore, unmodeled variations in system parameters (such as mass or inertia) during flight can cause significant stabilization errors to occur.

The need for an accurate nonlinear model of quadrotor dynamics can be prevailed or overcame the previous shortcoming on the model by using adaptive methods that can react to and correct errors in model parameter estimates, modify parameter estimates when they change and also adjust for external disturbances. Linear adaptive methods such as model reference adaptive control have been suggested [13].

However, as for almost all linear methods, the accomplished trajectory of the quadrotor is restricted due to the assumption of linearization. The paper in [14], suggested that an adaptive backstepping method. This approach was extended to include inertia parameters in the adaptation law. Indirect methods correct parameter errors based on the difference between the expected and actual plant outputs, but do not explicitly

correct the model parameters [15]. However autonomous constructing and grasping using quadrotors uses indirect adaptive methods, such as the least-squares method (for mass) as designed by Kumar *et al*. [16].

In [17], R. Naldi *et al*. proposed feedback controllers based on a hierarchical control algorithm for attitude, which is managed by means of a hybrid controller so as to overcome the well-known topological constraint, employed as a virtual input to stabilize the position of the aircraft.

The work in [18], designed backstepping controller with integral action and suggested a single tool to design attitude, altitude and position control. The researcher considered the rotor dynamics approximated to first order transfer function but did not consider the aerodynamics disturbances.

A Kalman filter is used for state estimation and noise filtering in [19]. Linear control techniques such as LQR, PID as well as modern robust mixed-sensitivity H_1 and μ-synthesis are employed and make comparison with each other in terms of flight reference trajectory tracking and parametric and also model uncertainty. Finally, the researcher suggested as future work to make disturbance rejection controller like SMC and backstepping.

Five years ago, at AAiT Ruth in [20], proposed quadrotor controller by ignoring the effect of aerodynamic effects and considering the quadrotor at hovering position only using LQR (linear quadratic regulator) and PID controllers but it works only at equilibrium point or during hovering. The researcher uses pole placement technique to design a state feedback by shifting poles in the real part to the desired places. The problem on this work was the controller controls the dynamics at hover or equilibrium point only ignoring the aerodynamic effects and other disturbances. But still, there is lack of accurate reference tracking.

In [21], C. Wang designed a hierarchical nonlinear adaptive control structure for quadrotor to track 3D reference trajectory affected with payload and time-varying wind gust variation disturbance. The problem was that the researcher ignoring the gyroscopic effect of quadrotor and its rotors, got lower controller performance.

N. Hadi Abbas in [22], used tuning of PID controllers for quadcopter system using hybrid memory based gravitational search algorithm – particle swarm optimization the problem on this work was the ignorance of aerodynamic effects from the model,

In [23], Y. Bouzid *et al.* worked on "trajectory tracking control of quadrotor UAV" with on-line disturbance compensation using model-free control (MFC) principle to deal with the unknown part of the system (i.e. unmodeled dynamics, disturbances, etc.). The result obtained was good but the work didn't consider rotor and quadrotor moment effects.

In this work aerodynamic and moment effects created by rotor dynamics and external disturbances that are omitted in many literatures are given due attention. Moreover, using nonlinear sliding mode control is used to improve robustness and chattering effect is minimized to improve trajectory tracking performances.

Chapter Three

Mathematical Modelling and Control System Design

3.1. Mathematical Modelling of Quadrotor

In this section the quadrotor geometrical structure and its reference frame are discussed and also its nonlinear dynamic model are obtained.

3.1.1. Kinematics

In this section the quadrotor geometrical structure and its reference frame are discussed as follows. Any analysis of the nonlinear system dynamics starts from kinematic study which defines the admissible configurations and velocities of the system. The kinematics of a rigid body deals with its possible configurations structure and allowable or permissible velocities without considering what causes the motion. The relationship between the forces and torques that cause the motion is referred to as dynamics.

The location of a rigid body in space can be expressed by the position and orientation of a reference frame attached to the rigid body with respect to the inertial frame called rigid body transformations.

3.1.1.1. Reference Frames

A reference frame is a set of points in space for which the distance between any two points is fixed at all times [24]. Even though, as it can be seen from this definition, any choice of the three or more non-collinear points can be used as a frame of reference called reference frame. The simplest way to study a reference frame is to think of a rigid body. In this context, here reference frame are used, first to identify a reference frame with a rigid body and then to study the motion of this reference frame with respect to an inertial reference frame. Rigid bodies and reference frames are thus used interchangeably. Therefore, a two-coordinate systems are required. There is the body frame system which is attached to the quadrotor at its center of gravity and the earth frame system which is fixed to the earth and it is sometimes refer to as an inertial coordinate system.

In this research work, the studied quadrotor rotorcraft is detailed with its body and inertial frames F_b (x^b; y^b; z^b) and F_i (x^i; y^i; z^i) respectively as shown Fig. 3.1.

The model partitions naturally into translational and rotational coordinates [25].

$$\xi = (x; y; z) \in R^3, \qquad \eta = (\phi; \theta; \psi) \in R^3 \tag{3.1}$$

Where $\xi = (x; y; z)$ represent the position vector of the center of mass of the quadrotor relative to the fixed inertial frame. $\eta = (\phi; \theta; \psi)$ denotes the rotational dynamics of the quadrotor given by the Euler angles ϕ, θ and ψ or it is called angular position vector.

The following figure shows quadrotor configuration and how it works.

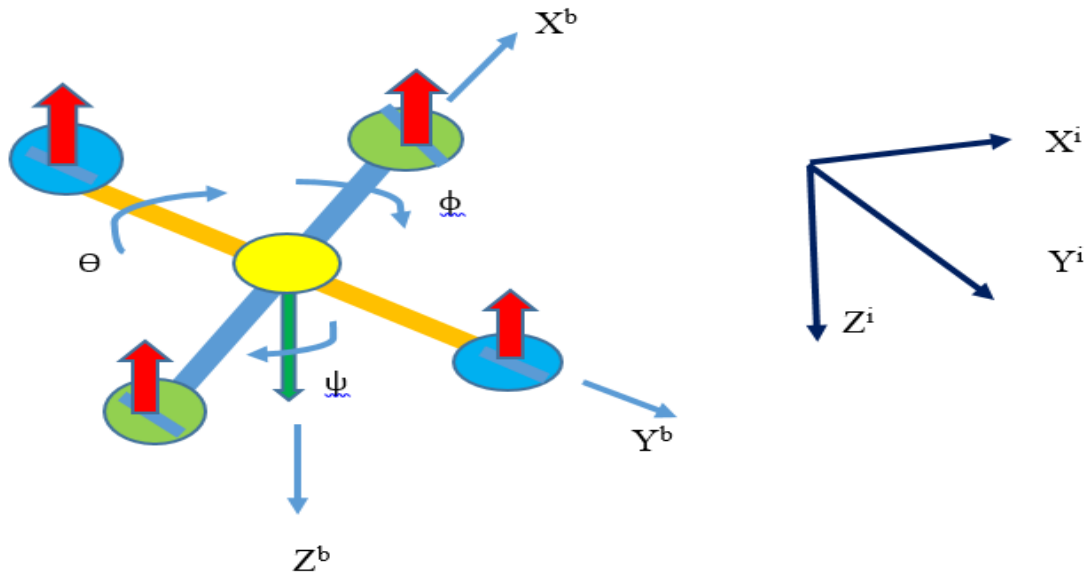

Fig. 3.1: Mechanical structure and configuration of the quadrotor with body and inertial frame

3.1.2. Rotational Matrix

Quadrotor employs different control mechanism such as roll, pitch, and yaw which in most cases are represented by Euler angle of rotation around the center of the quadrotor. To bring the body fixed frame into coincidence with the earth fixed frame the rotation matrix are considered. It describes the transformation earth-fixed coordinate to body-fixed coordinates by using rotational matrix [24].

The attitude system can be derived by rotating the body frame around the z axis of the by yaw angle ψ, followed by rotating around the y-axis by the pitch angle θ and finally by rotating around the x-axis by the roll angle ϕ with respect to fixed reference frame**.** In order to avoid the system singularities (loss of degree of freedom) it is sufficient to assume [10]**.**

$$-\pi/2 < \phi < \pi/2; -\pi/2 < \theta < \pi/2; -\pi < \psi < \pi \tag{3.2}$$

And the rotation matrix is derived as follows.

$$R(x,\phi)=\begin{bmatrix}1 & 0 & 0\\ 0 & c_\phi & s_\phi\\ 0 & -s_\phi & c_\phi\end{bmatrix};\ R(y,\theta)=\begin{bmatrix}c_\theta & 0 & -s_\theta\\ 0 & 1 & 0\\ s_\theta & 0 & c_\theta\end{bmatrix};\ R(z,\psi)=\begin{bmatrix}c_\psi & s_\psi & 0\\ -s_\psi & c_\psi & 0\\ 0 & 0 & 1\end{bmatrix} \quad (3.3)$$

The orientation of the quadrotor is given by the rotation matrix R: - $F_i \rightarrow F_b$, which depends on the three Euler angles (ϕ; θ; ψ) and defined by the following equation.

The rotation about ZYX or R_{zyx} and its transpose matrix R_{xyz}^T

$$R_{xyz} = R(z,\psi)\,R(y,\theta)\,R(x,\phi)$$

$$= \begin{bmatrix} c_\phi c_\theta & c_\theta s_\psi & -s_\theta \\ s_\phi s_\theta c_\psi - c_\phi s_\psi & s_\phi s_\theta s_\psi + c_\phi c_\psi & s_\phi c_\theta \\ c_\phi s_\theta c_\psi + s_\phi s_\psi & c_\phi s_\theta s_\psi - s_\phi c_\psi & c_\phi c_\theta \end{bmatrix} \quad (3.4)$$

$$R_{xyz}^T = \begin{bmatrix} c_\phi c_\theta & s_\phi s_\theta c_\psi - c_\phi s_\psi & c_\phi s_\theta c_\psi + s_\phi s_\psi \\ c_\theta s_\psi & s_\phi s_\theta s_\psi + c_\phi c_\psi & c_\phi s_\theta s_\psi - s_\phi c_\psi \\ -s_\theta & s_\phi c_\theta & c_\phi c_\theta \end{bmatrix} \quad (3.5)$$

One of the properties of the rotational matrix is that its inverse and its transpose are identical. In order to transform any linear quantity from earth frame to body frame, rotation matrices are used.

3.1.3. Assumptions for Quadrotor Modelling and its Operation

The nonlinear dynamic models of a quadrotor will be obtained based on Newton-Euler formalism. It can be derived using Lagrangian method, but it is little complex. The following assumptions are considered [5] [18].

- The structure is rigid and symmetrical.
- The center of gravity of the quadrotor coincides with the body fixed frame origin.
- The propellers are rigid.
- Thrust and Drag force are proportional to the square of speed of propeller.

The adjacent rotors of quadrotor are moving in opposite direction to produce thrust force as shown Fig. 3.2.

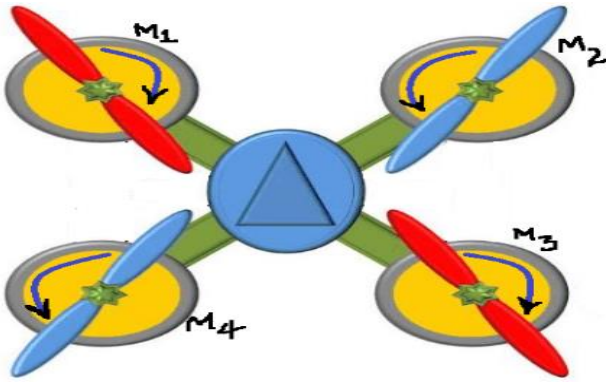

Fig. 3.2: Alignment of quadrotor motor rotating direction to produce thrust force

From Fig. 3.2 above, M_1 and M_3 rotating in clockwise (CW) and M_2 and M_4 rotating in counter clockwise (CCW) direction to produce the required thrust force. Quadrotor has four rotors that produce thrust force which are proportional to square of rotor angular speed.

The gyroscopic effects and the aerodynamic torques tend to oppose the flight quadrotor because of the mechanical design of the quadrotor and its modeling. The total thrust force F is the sum of individual thrust of each motor [25].

$$F = F_1 + F_2 + F_3 + F_4 = \sum_{i=1}^{4} F_i \qquad (3.6)$$

During quadrotor flight, it is subjected to external forces like the gusts of wind, gravity, viscous friction and others self-generated forces such as the thrust and drag. In addition to that, external torques are provided mainly by the trust of rotors and the drag on its body and propellers. Moments generated by gyroscopic effects of motors also affect it.

According to [26] [27] [28], the thrust force generated by the i^{th} rotor of the quadrotor is given by:

$$F_i = \frac{1}{2}\rho A C_t r^2 w_i^2 = b w_i^2 \text{ , where } b = \frac{1}{2}\rho A C_t r^2 \text{ (constant)} \qquad (3.7)$$

Where ρ is density of air [1.225 kg/m3], A is sectional area of propellers in m^2; r is radius of propeller m; C_t is aerodynamic thrust coefficient and w_i is angular speed of the i^{th} rotors in rad/s.

The aerodynamic drag torque, caused by the drag force at the propeller of the i^{th} rotor that opposed the torque of the motor, is defined as follows:

$$\tau_d = \frac{1}{2}\rho A C_d r^2 w_i^2 = d w_i^2 \text{ , where } d = \frac{1}{2}\rho A C_d r^2 \text{ (constant)} \qquad (3.8)$$

Where C_d is aerodynamic drag coefficient.

3.1.3.1. The Roll Torque

The roll torque (τ_ϕ) is responsible for the turning effect of the propellers during rotation when the quadrotor moving in the rotational phi (ϕ) direction as shown Fig. 3.3. That is directly proportional to the difference of thrust force generated by the 2nd and 4th motors (F_4 - F_2) [26]-[28].

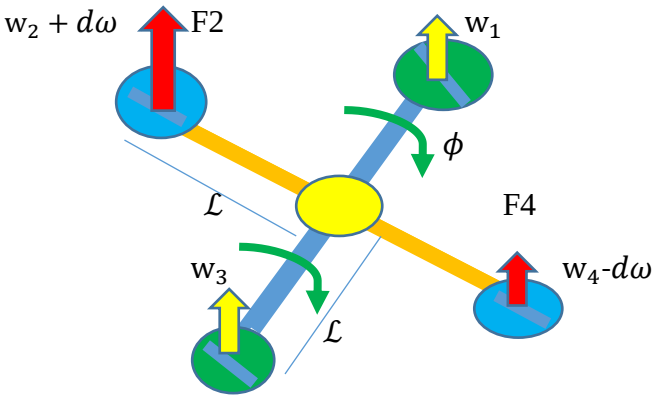

Fig. 3.3: Roll movement torque $\{w_2 > w_4 < (w_1 = w_3)\}$

In the figure above $d\omega$ is small change of angular speed. The roll torque is given by:

$$\tau_\phi = \mathcal{L}(F_4 - F_2) \tag{3.9}$$

Where $\mathcal{L}$ is the distance from the center of each rotors to center of the gravity (the quadrotor object center) [26]-[28].

3.1.3.2. The Pitch Torque

This torque (τ_θ) is turning effect of propellers during rotation when the quadrotor is moving in the rotational theta (Θ) axis as shown Fig. 3.4. It is directly proportional to the difference of thrust force generated by the 3rd and 1st motors ($F_3 - F_1$) [26]-[28].

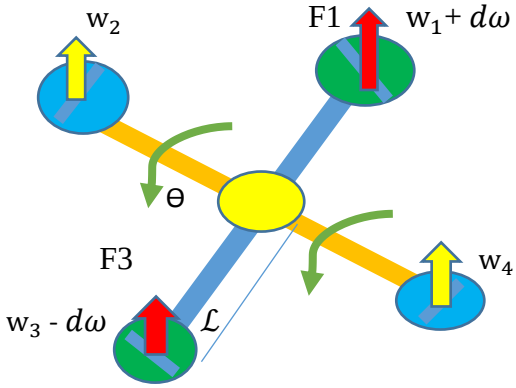

Fig. 3.4: Pitch movement torque $\{w_1 > w_3 < (w_2 = w_4)\}$

The roll torque is given by: $\tau_\theta = \mathcal{L}(F_3 - F_1)$, (3.10)

3.1.3.3. The Yaw Torque

Yaw torque (τ_ψ) is turning effect of propeller during rotation when the quadrotor is flying on rotational psi (ψ) direction as shown Fig. 3.5. This torque is used to control the heading of the quadrotor. That is directly proportional to the difference of thrust force generated by all the motors (F1 - F2 + F3 - F4) [27] [28].

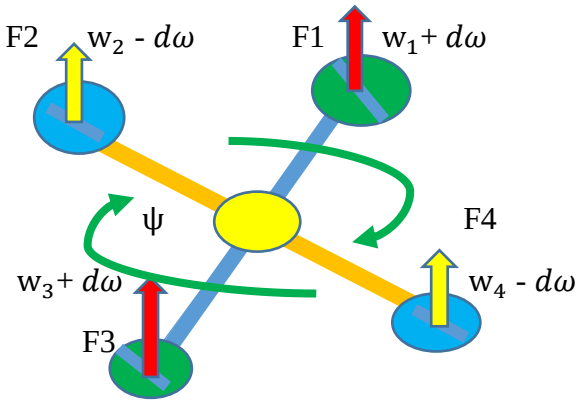

Fig. 3.5: Yawing movement torque $\{(w_4 = w_2) < (w_1 = w_3)\}$

$$\tau_\psi = c\,(F1 - F2 + F3 - F4) \tag{3.11}$$

Where c is constant coefficient (b/d).

The moment about the Z axis, which is the thrust force of the rotor, does not causes a moment rather the rotor rotation in relation with the rotor speed causes the moment seen the above Fig. 3.5.

If all rotor speeds are equals (i.e.$w_1 = w_2 = w_3 = w_4$), constant thrust is produced making the movement vertically in the z axis alone.

3.1.4. Moment and Force Equation

Gyroscopic Effect: The gyroscopic moment is induced on the quadrotor system from the four rotors and rigid body (quadrotor object). The gyroscopic effect of rotors is smaller than the one caused by the rigid body rotation [29].

Therefore, there are two gyroscopic effects of torque, these are due to the motion of the propellers(M_{gp}) and the quadrotor body (M_{gb}) [27] [28], given by:

$$M_{gp} = \sum_{i=1}^{4} \Omega \times \left[0, 0, \bar{J}_r(-1)^{i+1} w_i\right]^T \tag{3.12}$$

$$M_{gb} = \Omega \times J\Omega; \tag{3.13}$$

$$J = \begin{bmatrix} I_{xx} & 0 & 0 \\ 0 & Iyy & 0 \\ 0 & 0 & Izz \end{bmatrix} = \begin{bmatrix} I_{\chi} & 0 & 0 \\ 0 & Iy & 0 \\ 0 & 0 & Iz \end{bmatrix} \quad (3.14)$$

Since quadrotor geometry is symmetric, $I_{xy} = I_{xz} = I_{yx} = I_{yz} = I_{zx} = I_{zy} = 0$

Where Ω is vector of angular velocity in fixed earth frame

$$\Omega = \left[\dot{\Phi}, \dot{\theta}, \dot{\Psi}\right]^T \quad (3.15)$$

J is the moment inertia matrix of the quadrotor, I_x, I_y and I_z denoting the moment inertias of the x-axis, y-axis and z-axis of the quadrotor, respectively. J_r denotes the vertical or z-axis inertia of the rotors.

$$\Omega_r = w_1 - w_2 + w_3 - w_4 = (-1)^{i+1} w_i \quad (3.16)$$

Ω_r is the overall residual rotor angular velocity of quadrotor.

The cross product results of above equation (3.9 and 3.10):

$$M_{gp} = \left[\dot{\Phi}, \dot{\theta}, \dot{\Psi}\right]^T \text{ x } [0, 0, \bar{J}_r \Omega_r]^T = \begin{bmatrix} \dot{\theta} \bar{J}_r \Omega_r \\ -\dot{\Phi} \bar{J}_r \Omega_r \\ 0 \end{bmatrix} \quad (3.17)$$

$$M_{gb} = \Omega \text{ x } J\Omega = \left[\dot{\Phi}, \dot{\theta}, \dot{\Psi}\right]^T \text{ x } \begin{bmatrix} I_{\chi} & 0 & 0 \\ 0 & Iy & 0 \\ 0 & 0 & Iz \end{bmatrix} \left[\dot{\Phi}, \dot{\theta}, \dot{\psi}\right]^T$$

$$= \begin{bmatrix} \dot{\theta}\dot{\Psi}(Iz - Iy) \\ \dot{\Phi}\dot{\Psi}(Ix - Iz) \\ \dot{\theta}\dot{\Phi}(Iy - Ix) \end{bmatrix} \quad (3.18)$$

The quadrotor is controlled by independently varying the speed of the four rotors. Hence, these control commands or inputs are defined as follows: (N.B: Thrust and torque are proportional to the square of rotor angular speed.)

$$F = \sum_{i=1}^{4} F_i = b \sum_{i=1}^{4} w_i^2 \; ; \; F_1 = b w_1^2, F_2 = b w_2^2, F_3 = b w_3^2, F_4 = b w_4^2 \quad (3.19)$$

Control input for the dynamics as assigned in [25] given as follows:

$$U1 = Fi = \sum_{i=1}^{4} F_i = b \sum_{i=1}^{4} w_i^2 = F_1 + F_2 + F_3 + F_4 = F \quad (3.20)$$

$$U2 = \tau_{\phi} = \mathcal{L}(F_4 - F_2) = \mathcal{L} b (w_4^2 - w_2^2) \quad (3.21)$$

$$U3 = \tau_{\theta} = \mathcal{L}(F_3 - F_1) = \mathcal{L} b (w_3^2 - w_1^2) \quad (3.22)$$

$$U4 = \tau_{\psi} = c\,(F_1 - F_2 + F_3 - F_4) = d\,(w_1^2 - w_2^2 + w_3^2 - w_4^2); \quad d = cb \quad (3.23)$$

Where b and d are greater than zero and depends on air density, geometry and lift and drag coefficients of the propellers.

In matrix form it becomes

$$\begin{bmatrix} U_1 \\ U_2 \\ U_3 \\ U_4 \end{bmatrix} = \begin{bmatrix} b & b & b & b \\ 0 & -\mathcal{L}b & 0 & \mathcal{L}b \\ -\mathcal{L}b & 0 & \mathcal{L}b & 0 \\ d & -d & d & -d \end{bmatrix} \begin{bmatrix} w_1^2 \\ w_2^2 \\ w_3^2 \\ w_4^2 \end{bmatrix} = \begin{bmatrix} F \\ \tau_\phi \\ \tau_\theta \\ \tau_\psi \end{bmatrix} \tag{3.24}$$

From (3.24) matrix angular speed can be calculated as the as follow:

$$\begin{bmatrix} b & b & b & b \\ 0 & -\mathcal{L}b & 0 & \mathcal{L}b \\ -\mathcal{L}b & 0 & \mathcal{L}b & 0 \\ d & -d & d & -d \end{bmatrix}^{-1} \begin{bmatrix} U_1 \\ U_2 \\ U_3 \\ U_4 \end{bmatrix} = \begin{bmatrix} w_1^2 \\ w_2^2 \\ w_3^2 \\ w_4^2 \end{bmatrix} \tag{3.25}$$

3.1.5. Modeling with Newton-Euler Formalism

While using the Newton-Euler formalism for modeling the low leads the following equations. From Newton's law, the total force applied to a system equivalent to the product of mass and acceleration [25]-[28].

$$m\ddot{\xi} = F_{th} - F_d - F_g \tag{3.26}$$

$$\ddot{\xi} = \begin{bmatrix} \ddot{X} \\ \ddot{y} \\ \ddot{z} \end{bmatrix} \tag{3.27}$$

Where m is total mass of the quadrotor, $\ddot{\xi}$ translational acceleration vector, and F_d is air drag force which resists to the quadrotor motion.

$$F_d = \text{diag}\,[k_1, k_2, k_3]\dot{\xi}^T$$

$$= \begin{bmatrix} k_1 & 0 & 0 \\ 0 & k_2 & 0 \\ 0 & 0 & k_3 \end{bmatrix} [\dot{x}, \dot{y}, \dot{z}]^T \tag{3.28}$$

Diag $[k_1, k_2, k_3]$ are aerodynamic drag force coefficients and $\dot{\xi}$ is speed vector for translational dynamics.

F_g is the force of gravity towards the earth; $\quad F_g = \begin{bmatrix} 0 \\ 0 \\ mg \end{bmatrix}$, (3.29)

Where g is gravitational acceleration.

F_{th} is the thrust force produced by the four rotors in the inertial frame transformed from body frame and the relation is described by rotational matrix as follows [26]:

$$F_{th}=R_{xyz}^{T}\begin{bmatrix}0\\0\\F\end{bmatrix}=\begin{bmatrix}F(c_\phi s_\theta c_\psi + s_\phi s_\psi)\\F(c_\phi s_\theta s_\psi - s_\phi c_\psi)\\F(c_\phi c_\theta)\end{bmatrix} \quad (3.30)$$

So, from the above equation (3.25) the following translational dynamics of quadrotor can be obtained.

$$\begin{aligned}\ddot{x} &= \frac{1}{m}\left(\left(c_\phi s_\theta c_\psi + s_\phi s_\psi\right)U_1 - k_1\dot{x}\right)\\ \ddot{y} &= \frac{1}{m}\left(\left(c_\phi s_\theta s_\psi - s_\phi c_\psi\right)U_1 - k_2\dot{y}\right)\\ \ddot{z} &= \frac{1}{m}\left(\left(c_\phi c_\theta\right)U1 - k_3\dot{z}\right) - g\end{aligned} \quad (3.31)$$

From Euler torque equation the resultant torque is given by [25, 26],

$$J\dot{\Omega} = M - M_{gp} - M_{gb} - M_a \quad (3.32)$$

$$M=\begin{bmatrix}\tau_\phi\\\tau_\theta\\\tau_\psi\end{bmatrix} \quad (3.33)$$

$$\dot{\Omega}=\begin{bmatrix}\ddot{\phi}\\\ddot{\theta}\\\ddot{\Psi}\end{bmatrix} \quad \text{are angular acceleration vector} \quad (3.34)$$

M_a is the torque resulting from the aerodynamic frictions

$$M_a=\begin{bmatrix}k_4 & 0 & 0\\0 & k_5 & 0\\0 & 0 & k_6\end{bmatrix}\begin{bmatrix}\dot{\phi}^2\\\dot{\theta}^2\\\dot{\psi}^2\end{bmatrix} \quad (3.35)$$

Diag $[k_4, k_5, k_6]$ are the aerodynamic drag torque coefficients which are positive constants [26]. M_{gp} and M_{gb} are described in equation (3.17) and (3.18) respectively.

From equation (3.31) rotational (Euler dynamics) can be derived the as follow:

$$\begin{aligned}\ddot{\phi} &= \frac{1}{I_x}\left(U_2 - k_4\dot{\phi}^2 - J_r\Omega_r\dot{\theta} + (Iy - Iz)\dot{\theta}\dot{\psi}\right)\\ \ddot{\theta} &= \frac{1}{I_y}\left(U_3 - k_5\dot{\theta}^2 + J_r\Omega_r\dot{\phi} + (Iz - Ix)\dot{\phi}\dot{\psi}\right)\\ \ddot{\psi} &= \frac{1}{I_z}\left(U_4 - k_6\dot{\psi}^2 + (Ix - Iy)\dot{\theta}\dot{\phi}\right)\end{aligned} \quad (3.36)$$

3.1.6. State Space Model Representation

Writing the acquired mathematical model into a state space form simplifies the implementation of control technique.

$$\dot{X} = f(X, U) \tag{3.37}$$

X is state vector, U is control input vector

$$X = \left[\phi, \dot{\phi}, \theta, \dot{\theta}, \psi, \dot{\psi}, x, \dot{x}, y, \dot{y}, z, \dot{z}\right]^T \in R^{12} \tag{3.38}$$

State vector can be written as

$$X = [x_1\ x_2\ x_3\ x_4\ x_5\ x_6\ x_7\ x_8\ x_9\ x_{10}\ x_{11}\ x_{12}]^T \in R^{12} \tag{3.39}$$

$$U = [U_1\ U_2\ U_3\ U_4]^T$$

$$X = \begin{pmatrix} x_{1=\phi} \\ x_{2=\dot{\phi}} \\ x_{3=\theta} \\ x_{4=\dot{\theta}} \\ x_{5=\psi} \\ x_{6=\dot{\psi}} \\ x_{7=x} \\ x_{8=\dot{x}} \\ x_{9=y} \\ x_{10=\dot{y}} \\ x_{11=z} \\ x_{12=\dot{z}} \end{pmatrix} \tag{3.40}$$

The state-space representation of the studied quadrotor is obtained as follows:

$$\begin{aligned}
&\dot{x}_1 = x_2, \quad \dot{x}_2 = c_1 x_4 x_6 + c_2 x_2^2 + c_3 \Omega_r x_4 + b_1 U_2 \\
&\dot{x}_3 = x_4, \quad \dot{x}_4 = c_4 x_2 x_6 + c_5 x_4^2 + c_6 \Omega_r x_2 + b_2 U_3 \\
&\dot{x}_5 = x_6, \quad \dot{x}_6 = c_7 x_2 x_4 + c_8 x_6^2 + b_3 U_4 \\
&\dot{x}_7 = x_8, \quad \dot{x}_8 = c_9 x_8 + \frac{1}{m}\left(c_\phi s_\Theta c_\psi + s_\phi s_\psi\right) U_1 \\
&\dot{x}_9 = x_{10}, \quad \dot{x}_{10} = c_{10} x_{10} + \frac{1}{m}\left(c_\phi s_\Theta s_\psi - s_\phi c_\psi\right) U_1 \\
&\dot{x}_{11} = x_{12}, \quad \dot{x}_{12} = c_{11} x_{12} + \frac{1}{m}\left(c_\phi c_\Theta\right) U_1 - g
\end{aligned} \tag{3.41}$$

The relation between position (x, y), altitude (z) and rotational (ϕ, Θ, ψ) dynamics are represents by

$$\begin{aligned}
U_x &= \left(c_\phi s_\Theta c_\psi + s_\phi s_\psi\right) = c_{x_1} s_{x_3} c_{x_5} + s_{x_1} s_{x_5} \\
U_y &= \left(c_\phi s_\Theta s_\psi - s_\phi c_\psi\right) = c_{x_1} s_{x_3} s_{x_5} - s_{x_1} c_{x_5}
\end{aligned} \tag{3.42}$$

Where $c_1 = \frac{I_y - I_z}{I_x}$; $c_2 = -\frac{k_4}{I_x}$; $c_3 = -\frac{J_r}{I_x}$; $c_4 = \frac{I_z - I_x}{I_y}$; $c_5 = -\frac{k_5}{I_y}$; $c_6 = \frac{J_r}{I_y}$; $c_7 = \frac{I_x - I_y}{I_z}$

$c_8 = -\frac{k_6}{I_z}$; $c_9 = -\frac{k_1}{m}$; $c_{10} = -\frac{k_2}{m}$; $c_{11} = -\frac{k_3}{m}$; $b_1 = \frac{1}{I_x}$; $b_2 = \frac{1}{I_y}$; $b_3 = \frac{1}{I_z}$

To extract the reference or desired trajectory for phi and theta (ϕ_d, θ_d) from virtual loop (x and y dynamics) Ux and Uy are used. From equation (3.42) the desired roll and pitch trajectories are extracted from designed controller Ux and Uy. Where

$$U_x = (c_{\phi_d} s_{\theta_d} c_\psi - s_{\phi_d} s_\psi) \text{ and } U_y = (c_{\phi_d} s_{\theta_d} s_\psi - s_{\phi_d} c_\psi) \quad (3.43)$$

In vector forms it becomes

$$\begin{bmatrix} U_y \\ U_x \end{bmatrix} = \begin{bmatrix} s_\psi & -c_\psi \\ c_\psi & s_\psi \end{bmatrix} \begin{bmatrix} c_{\phi_d} s_{\theta_d} \\ s_{\phi_d} \end{bmatrix}$$

$$\begin{bmatrix} c_{\phi_d} s_{\theta_d} \\ s_{\phi_d} \end{bmatrix} = \begin{bmatrix} s_\psi & -c_\psi \\ c_\psi & s_\psi \end{bmatrix}^{-1} \begin{bmatrix} U_y \\ U_x \end{bmatrix}$$

By starting from second row ϕ_d and then θ_d can be calculated as follows:

$$\begin{bmatrix} \phi_d \\ \theta_d \end{bmatrix} = \begin{bmatrix} \arcsin(U_x s_\psi - U_y c_\psi) \\ \arcsin((U_x c_\psi - U_y s_\psi)/c_{\phi_d}) \end{bmatrix} \quad (3.44)$$

3.1.7. Open Loop Model Verification

The open loop model without applying controller is verified using Matlab/Simulink block as shown Fig. 3.6, to check the system validity constant speed is assigned for the rotors and then the block is simulated.

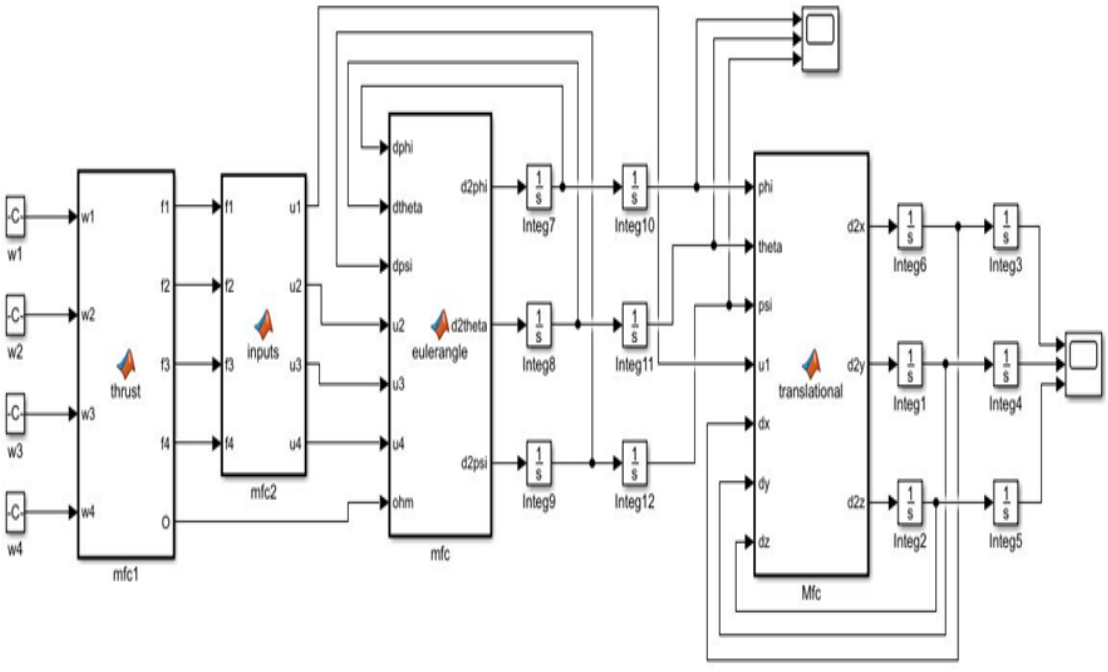

Fig. 3.6: Open loop Simulink block diagram

The open loop dynamic model shows that the effect of the input on the output state by using rotor speed for calculating input U1, U2, U3, and U4 or thrust force, roll torque, pitch torque and yaw torque respectively. The model simulation is done at different speeds depending on above equations (3.20 - 3.23) for all dynamics.

Table 3.1: Quadrotor model parameters used for simulation purpose

Parameter	**Value and unit**
Lift coefficient (b)	$2.984*10^{-5}$ N s^2/rad^2
Drag coefficient (d)	$3.3*10^{-7}$ Nm s^2/rad^2
Total mass (m)	0.823 kg
Arm length (l)	0.35 m
Motor inertia (J_r)	$2.8385*10^{-5}$ kg m^2
Aerodynamic friction coeffs ($K_{1,2,3}$)	0.3729
Quadrotor moment of inertia (Ix,Iy,Iz)	0.005, 0.005, 0.01 in (kg m^2) resp.
Translational aerodynamics drag coeffs ($K_{4,5,6}$)	$5.56*10^{-4}$
Gravitational acceleration(g)	9.8 m/s^2

The constant parameter value listed in Table 3.1 are taken from literature. The moment of inertial constants can be calculated from physical model of quadrotor and the aerodynamics friction coefficient are depend on the air condition.

Fig. 3.7 shows that all rotor speeds are the same, only the input signal U1 is affecting the altitude z-dynamic. That means the motion of the quadrotor is only along the z-axis.

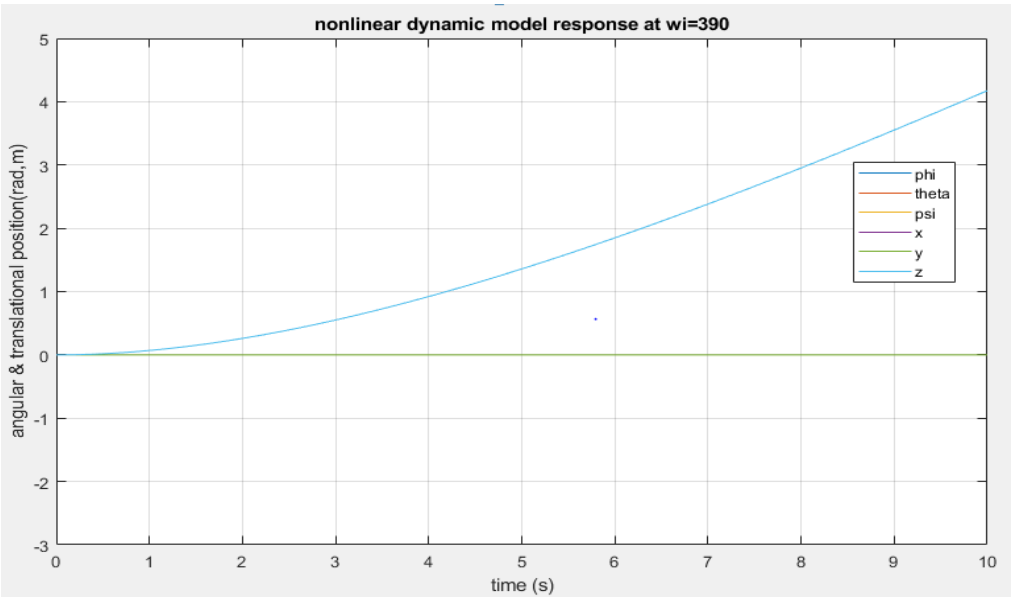

Fig. 3.7: Simulation result at $w_1=w_2=w_3=w_4=390$ in (rad/s)

The result in Fig. 3.8 shows the quadrotor is at equilibrium point, all rotor speeds are zero. Which is when the gravitational force alone affected the quadrotor altitude (z).

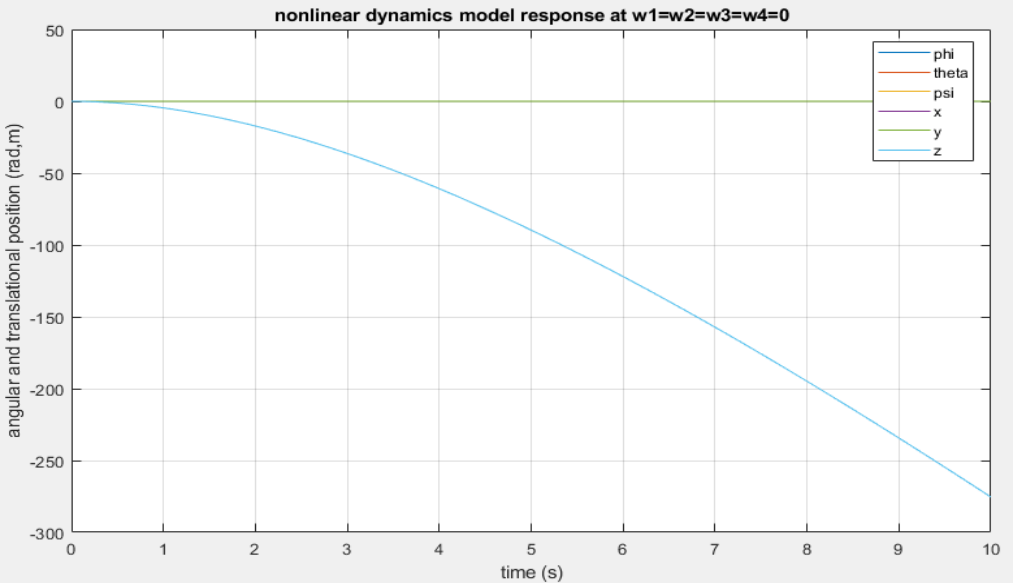

Fig. 3.8: Simulation result on z-dynamics at $w_1=w_2=w_3=w_4=0$ in (rad/s)

The simulation result in Fig. 3.9 below shows that the pitch (theta) torque is affecting the translational dynamics state output (x and z) and Θ dynamics. The input U3 affects the theta dynamics or state that is called pitch dynamics.

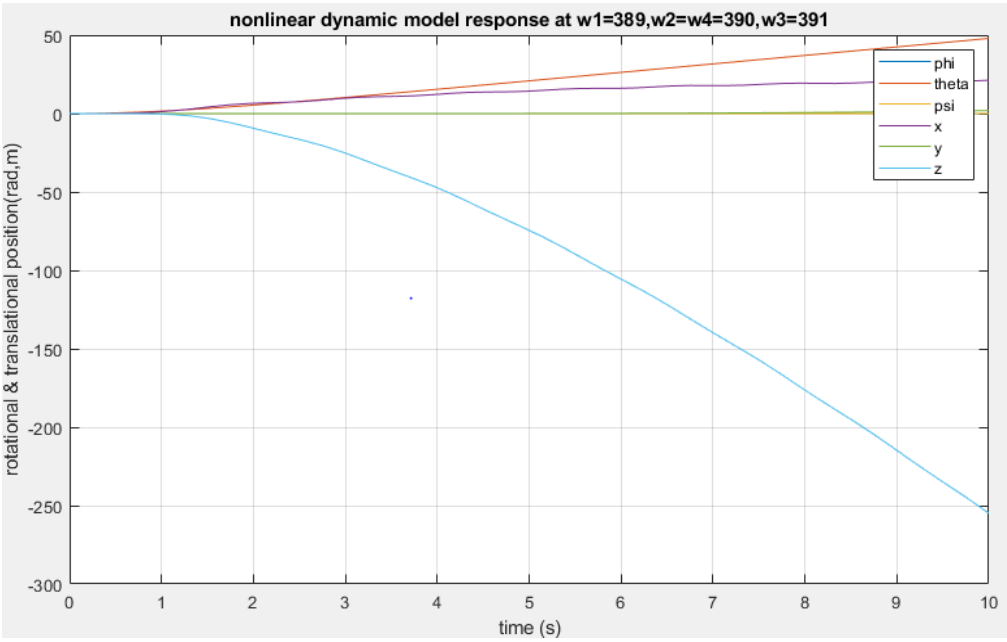

Fig. 3.9: Simulation of pitch torque effect at $w_1=389$, $w_2=w_4=390$, $w_3=391$ in (rad/s)

The result in Fig. 3.10 shows that the roll (phi) torque affects the output state y, z and ϕ. Therefore, the roll torque affects the rotational roll dynamics.

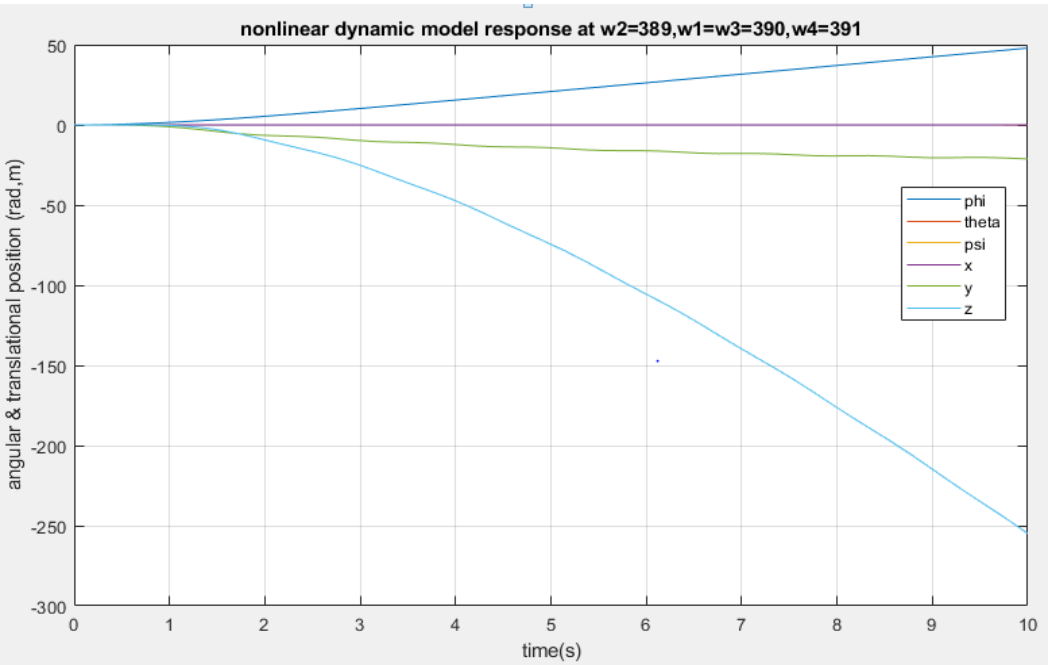

Fig. 3.10: Simulation of roll torque effect at w_1=w_3=390, w_2=389, w_4= 391 in (rad/s)

The result in Fig. 3.11 shows that the yaw torque affects the ψ and z dynamics, which implies U4 affects the angular position psi state, called yaw dynamics.

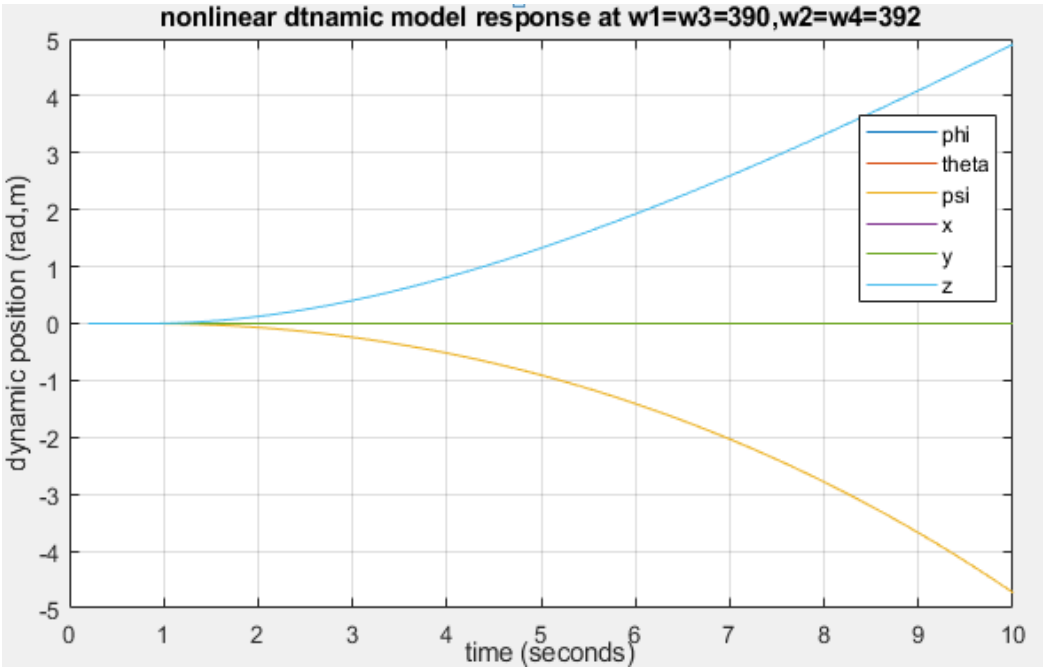

Fig. 3.11: Simulation result of yaw torque effect

3.2. Quadrotor Control System Design

In this work, SMC and fuzzy PID controllers are designed for controlling the nonlinear model of quadrotor UAV. The objective of using sliding mode controller is to control the three highly coupled translational dynamics (position and altitude) and Fuzzy PID controller is used for rotational or Euler dynamics (attitude and heading) of the quadrotor.

3.2.1. Sliding Mode Controller

3.2.1.1. Overview of Sliding Mode Controller

The sliding mode control (SMC) is a type of Variable Structure Control (VSC), done by attracting the system states towards a desired surface that is known as sliding surface. It is also a special version of an on-off control. The basic idea is that apply powerful control action when the system response deviates from the desired behavior. Sliding mode techniques are one of the best approaches to solving the control problems and are an area of increasing the researchers' interest. VSC with SMC was first proposed and elaborated in early 1950s in the Soviet Union by Emelyanov and several core researchers such as Utkins and Itkis [30]. In the last decade, significant interest on VSC and SMC have been shown in the control research community [30].

SMC has been applied including nonlinear systems, multi-input multi-output (MIMO) systems, infinite-dimension systems, discrete-time models, large-scale, and stochastic systems. The most eminent feature of SMC is it completely insensitive to parametric uncertainty and external disturbances during sliding mode [30] [31].

Basically, VSC utilizes a high-speed switching control law to drive the nonlinear plants state trajectory onto a desired and user-chosen surface in the state space and to maintain the plant's state trajectory on this surface for all subsequent time intervals. The sliding surface is called the switching surface because if the state trajectory of the plant is "above" the surface, a control path has one kind of gain and if the trajectory drops "below" the surface it has a different gain. During the process, the control systems structure varies from one form to another, thus earning the name VSC. To emphasize the important role of the sliding mode, the control is also called SMC [31].

The evolution of the state trajectory is divided into two parts [32]:

- From the initial state up to the intersection with the sliding surface, this is called "the reaching phase".
- From the intersection with the sliding surface up to the origin, this path is called "the sliding phase".

Suitably chosen and designed stabilizing control law keeps the system states on such a surface. For the choice of the sliding surface, the general form general form of equation was proposed by Stoline and Li in [26] [31].

$$S(x) = \left(\lambda_x + \frac{d}{dt}\right)^{f-1} e(x) \tag{3.45}$$

Where x is control variable or state vector, $e(x)$ is tracking error defined as $x_d - x$, λ_x is a positive constant that interprets the dynamics of the surface and f is the relative degree of the sliding mode controller.

3.2.1.2. Design of SMC for Quadrotor Nonlinear Dynamics

Condition, called attractiveness is the one under which the state trajectory will reach the sliding surface. Lyapunov based approach was used to access conditions to the sliding surface [25] [28]. It makes a positive scalar function called Lyapunov candidate function, given below in equation (3.46). For the system state variables and choose the control law that will decrease this function has been chosen:

$$\dot{V} < 0 \text{ with } V > 0 \tag{3.46}$$

For choosing Lyapunov function there is no general rule. In this work the positive Lyapunov candidate function for each single dynamics systems a suitable function is selected as:

$$V = \frac{1}{2}s^2 \tag{3.47}$$

These is clearly globally positive definite, to be stable the derivative $\dot{V} < 0$ that means:

$$\dot{V} = s\dot{s} < 0 \tag{3.48}$$

The objective is to attract the system state trajectories to reach the sliding surface and stay on it despite the presence of uncertainty.

Tracking error is the difference between desired value and the actual output value of the state is defined as follows:

$$e_{i+1} = \dot{e}_1 ; \quad e_i = x_{id} - x_i \text{ where } i=1, 2 \ldots 6 \tag{3.49}$$

According to reaching low "constant reaching low" the derivative of the switching surface to satisfy $\dot{V} = s\dot{s} < 0$ condition given by [30].

$$\dot{s}_i = -K_i \text{sgn}(s_i) \tag{3.50}$$

Where $K_i > 0$, denotes a constant rate.

$$\text{sgn}(s_i) = \begin{cases} 1, & s_i > 0 \\ 0, & s_i = 0 \\ -1, & s_i < 0 \end{cases} \tag{3.51}$$

Sliding mode based on reaching law includes reaching phase and sliding phase. The reaching phase drive system is to preserve a stable manifold and the sliding phase drive system guarantee sliding to equilibrium. This law constrains the switching parameter to reach the switching manifold ***s*** at a constant rate K_i. Its advantage is its simplicity. The value of K_i is too small, the reaching time will be too long. On the other hand, too large value of K_i will cause severe chattering, therefore, the choice of K_i value is decided by the success of SMC [30].

Equation (3.49) is used to choose the sliding surface function of the SMC, so that it possible to choose the sliding surface based on the tracking errors as shown below:

$$s_1 = \lambda_1 \phi_e + \dot{\phi}_e, \quad \phi_e = \phi_d - \phi = e_1 \tag{3.52}$$

Equation (3.52) is sliding surface and tracking error for roll dynamics, respectively.

$$s_2 = \lambda_2 \theta_e + \dot{\theta}_e, \quad \theta_e = \theta_d - \theta = e_2 \tag{3.53}$$

Equation (3.53) is sliding surface and tracking error for pitch dynamics, respectively.

$$s_3 = \lambda_3 \psi_e + \dot{\psi}_e, \quad \psi_e = \psi_d - \psi = e_3 \tag{3.54}$$

Equation (3.54) is sliding surface and tracking error for yaw dynamics, respectively.

$$s_6 = \lambda_6 z_e + \dot{z}_e, \quad z_e = z_d - z = e_6 \tag{3.55}$$

Equation (3.55) is sliding surface and tracking error for altitude dynamics, respectively.

The dynamic model divided into subsystem called internal dynamics and internal dynamics. The internal dynamics (X and Y) positon dynamics generates the desired angular position called roll and pitch (ϕ_d and Θ_d). The other subsystem is external dynamics include altitude, roll, pitch and yaw dynamics ($z, \phi\ \Theta, \psi$) [25].

The internal dynamics in case, it affects the quadrotor motion. However, it produces external disturbance which in turn affects the quadrotor motion. So that, the SMC is used stabilize this problem. The siding surface along this dynamics is given as follows:

$$s_x = \lambda_4 x_e + \dot{x}_e, \;\; x_e = x_d - x = e_4 \quad \text{for x axis dynamics} \tag{3.56}$$

$$s_y = \lambda_5 y_e + \dot{y}_e, \;\; y_e = y_d - y = e_5 \text{ for y axis dynamics} \tag{3.57}$$

Where $\lambda_{1,2,3,4,5,6}$ are greater than zero and must satisfy the Hurwitz condition.

Position Control: - Position controllers are used for controlling the translational X and Y (position) dynamics model of the quadrotor. Consider U_x and U_y are the orientations of U_1. It is responsible for the X and Y motion respectively.

Attitude Control: - Attitude controllers is used to the managed the rotational roll (phi) and pitch (theta) dynamics of the quadrotor.

Heading Control: - These controller manages the rotational psi dynamics that means left and right motion.

Altitude Control: - The altitude controller responsible for the height or vertical motion control along z-dynamics of the quadrotor.

Control law can be designed based on sliding surface of the position, altitude, attitude, and heading dynamics of the quadrotor (quadcopter).

a) SMC Design for Attitude Roll and Pitch Dynamics

The tracking error and switching surface for roll angle defined in equation (3.52) as

$\phi_e = \phi_d - \phi = e_1$; $s_1 = \lambda_1 \phi_e + \dot{\phi}_e$ respectively, the 1st derivative of the sliding surface is

$$\dot{s}_1 = \lambda_1 \dot{e}_1 + \ddot{e}_1 = \lambda_1 \dot{\phi}_e + \ddot{\phi}_e = \lambda_1 (\dot{\phi}_d - \dot{\phi}) + \ddot{\phi}_d - \ddot{\phi} \; ; \; \dot{s}_1 = -K_1 \text{sgn}(s_1) \tag{3.58}$$

From equation (3.36): $\ddot{\phi} = \dot{x}_2 = c_1 x_4 x_6 + c_2 x_2^2 + c_3 \Omega_r x_4 + b_1 U_2$ equate in equation (3.58) and U_2 can be calculated as follows:

$$U_2 = \frac{1}{b_1} \left[\ddot{\phi}_d - c_1 x_4 x_6 - c_2 x_2^2 - c_3 \Omega_r x_4 + \lambda_1 (\dot{\phi}_d - \dot{\phi}) - \dot{s}_1 \right],$$

$$U_2 = \frac{1}{b_1} [\ddot{x}_{1d} - c_1 x_4 x_6 - c_2 x_2^2 - c_3 \Omega_r x_4 + \lambda_1 \dot{e}_1 + K_1 \text{sgn}(s_1)] \tag{3.59}$$

Where $\dot{e}_1 = (\dot{\phi}_d - \dot{\phi}) = \dot{\phi}_e$

This design approach are repeating for all later system. So, for Pitch dynamics the pitch sliding surface and tracking error are as defined in equation (3.53):

$s_2 = \lambda_2 \theta_e + \dot{\theta}_e$, $\theta_e = \theta_d - \theta = e_2$, the pitch sliding surface and tracking error respectively, the derivative of sliding surface s_2 given by:

$$\dot{s}_2 = \lambda_2 \dot{e}_2 + \ddot{e}_2 = \lambda_2 \dot{\theta}_e + \ddot{\theta}_e = \lambda_2 (\dot{\theta}_d - \dot{\theta}) + \ddot{\theta}_d - \ddot{\theta}\,; \tag{3.60}$$

From equation (3.50) $\dot{s}_2 = -K_2 \mathrm{sgn}(s_2)$ and from equation (3.36).

$\ddot{\theta} = \dot{x}_4 = \ddot{x}_3 = c_4 x_2 x_6 + c_5 x_4^2 + c_6 \Omega_r x_2 + b_2 U_3$, equate from equation (3.60) and U_3 can be calculated as follows:

$$U_3 = \frac{1}{b_2}\left[\ddot{\theta}_d - c_4 x_2 x_6 - c_5 x_4^2 - c_6 \Omega_r x_2 + \lambda_2 (\dot{\theta}_d - \dot{\theta}) - \dot{s}_2\right], \ddot{\theta}_d = \ddot{x}_{3d},\ \dot{e}_2 = \dot{\theta}_d - \dot{\theta}$$

$$U_3 = \frac{1}{b_2}[\ddot{x}_{3d} - c_4 x_2 x_6 - c_5 x_4^2 - c_6 \Omega_r x_2 + \lambda_2 \dot{e}_2 + K_2 \mathrm{sgn}(s_2)] \tag{3.61}$$

b) SMC Design for Heading Yaw Dynamics

Sliding surface and tracking error along the yaw Euler axis of quadrotor as defined equation (3.54) $s_3 = \lambda_3 \psi_e + \dot{\psi}_e$, $\psi_e = \psi_d - \psi = e_3$ respectively. The derivative of the sliding surface s_3 is given by:

$$\dot{s}_3 = \lambda_3 \dot{e}_3 + \ddot{e}_3 = \lambda_3 \dot{\psi}_e + \ddot{\psi}_e = \lambda_3 (\dot{\psi}_d - \dot{\psi}) + \ddot{\psi}_d - \ddot{\psi}, \tag{3.62}$$

From equation (3.36) $\ddot{\psi} = \dot{x}_6 = \ddot{x}_5 = c_7 x_2 x_4 + c_8 x_6^2 + b_3 U_4$, insert in equation (3.62) and U_4 can be calculated as follows:

$$U_4 = \frac{1}{b_3}\left[\ddot{\psi}_d - c_7 x_2 x_4 - c_8 x_6^2 + \lambda_3 (\dot{\psi}_d - \dot{\psi}) - \dot{s}_3\right] \ , \ddot{\psi}_d = \ddot{x}_{5d}\ , \dot{e}_3 = \dot{\psi}_d - \dot{\psi}\ ,$$

$$U_4 = \frac{1}{b_3}[\ddot{x}_{5d} - c_7 x_2 x_4 - c_8 x_6^2 + \lambda_3 \dot{e}_3 + K_3 \mathrm{sgn}(s_3)] \tag{3.63}$$

c) SMC Design for Translational Z Dynamics

The relation between control input U_1 and gravitational force and aerodynamics force along the z-axis can be used to determine control low U_1.

$s_6 = \lambda_6 z_e + \dot{z}_e$, $e_z = z_d - z = e_6$ are the sliding surface and tracking error of the z axis dynamics respectively as defined in equation (3.55). The derivative of the switching surface is:

$$\dot{s}_6 = \lambda_6 \dot{e}_6 + \ddot{e}_6 = \lambda_6 \dot{z}_e + \ddot{z}_e = \lambda_6 (\dot{z}_d - \dot{z}) + \ddot{z}_d - \ddot{z}, \tag{3.64}$$

From the translational z dynamics in equation (3.31)

$\ddot{z} = \dot{x}_{12} = \ddot{x}_{11} = c_{11}x_{12} + \frac{1}{m}(c_\phi c_\Theta)U_1 - g$, equating from equation (3.64) and the altitude control input U_1 can be calculated as:

$U_1 = \frac{m}{c_\phi c_\Theta}[\ddot{z}_d - c_{11}x_{12} + g + \lambda_6\dot{e}_4 + K_6 sgn(s_6)]$, $\ddot{z}_d = \ddot{x}_{11d}$, $\dot{e}_6 = \dot{z}_e = \dot{z}_d - \dot{z}$,

$\phi = x_1$ and $\Theta = x_3$, therefore, the control input can be rewrite as:

$$U_1 = \frac{m}{c_{x1}c_{x3}}[\ddot{z}_d - c_{11}x_{12} + g + \lambda_6\dot{e}_6 + K_6 sgn(s_6)] \quad (3.65)$$

d) SMC Design for Translational X and Y Dynamics

The same approaches are used to design the control laws U_x and U_y for stabilization of the X and Y positions of the Quadrotor, respectively.

For the X dynamics the selected sliding surface and tracking error in equation (3.56) are $s_4 = \lambda_4 x_e + \dot{x}_e$, and $x_e = x_d - x = e_4$, respectively and its surface derivative is calculated as:

$$\dot{s}_4 = \lambda_4\dot{e}_4 + \ddot{e}_4 = \lambda_4\dot{x}_e + \ddot{x}_e = \lambda_4(\dot{x}_d - \dot{x}) + \ddot{x}_d - \ddot{x}\,, \dot{s}_4 = -K_4 sgn(s_4) \quad (3.66)$$

The translational dynamic modeling equation (3.31) for X dynamics are

$$\ddot{x} = \dot{x}_8 = \ddot{x}_7 = c_9x_8 + \frac{1}{m}(c_\phi s_\Theta c_\psi + s_\phi s_\psi)U_1 \text{ , where}$$

$$u_x = (c_\phi s_\Theta c_\psi + s_\phi s_\psi) = c_{x_1}s_{x_3}c_{x_5} + s_{x_1}s_{x_5} \quad (3.67)$$

So, the dynamics became $\ddot{x} = c_9x_8 + \frac{1}{m}u_xU_1$

After equating from equation (3.66), the desired X position controller U_x can be obtained as:

$$U_x = \frac{m}{U_1}[\ddot{x}_{7d} - c_9x_8 + \lambda_4\dot{e}_4 + K_4 sgn(s_4)] \quad (3.68)$$

For the Y position dynamics the selected switching function and tracking error in (3.57) are $s_5 = \lambda_5 y_e + \dot{y}_e$, & $y_e = y_d - y = e_5$, respectively and its surface derivative is given by:

$$\dot{s}_5 = \lambda_5\dot{e}_5 + \ddot{e}_5 = \lambda_5\dot{y}_e + \ddot{y}_e = \lambda_5(\dot{y}_d - \dot{y}) + \ddot{y}_d - \ddot{y}, \quad (3.69)$$

As discussed the translational dynamic modeling equation (3.31) for Y dynamics is

$\ddot{y} = \dot{x}_{10} = \ddot{x}_9 = c_{10}x_{10} + \frac{1}{m}(c_\phi s_\Theta s_\psi - s_\phi c_\psi)U_1$, where $\ddot{x}_{9d} = \ddot{y}_d$

Where $u_y = \left(c_\phi s_\Theta s_\psi - s_\phi c_\psi\right) = c_{x_1} s_{x_3} s_{x_5} - s_{x_1} c_{x_5}$ (3.70)

$\ddot{y} = c_{10} x_{10} + \frac{1}{m} U_y U_1$, equating from (3.70) the following control low is obtained.

$$U_y = \frac{m}{U_1}\left[\ddot{x}_{9d} - c_{10}x_{10} + \lambda_5 \dot{e}_5 + K_5 \mathrm{sgn}(s_5)\right] \quad (3.71)$$

3.2.2. Chattering Reduction

In sliding mode controller, chattering can be occurs due to the switch term $K_i \mathrm{sgn}(s_i)$, especially for a large disturbance, which will damage to system components such as actuators. It also causes excitation of unmodeled system dynamics. These may leads to instability of the system and also it may causes high power consumption and possible actuator may damage. Therefore it harder to apply sliding mode control on real systems. However, it is unavoidable in the real time application of SMC [30].

Several researches were made in order to reduce chattering by trying out different method like neural network, boundary condition around the surface, quasi and terminal SMC [33] [34]. The most common way to reduce this problem is to introduce a boundary layer around the sliding surface. These method is applied in this research.

(Utkin in 1999) suggests a SMC guideline for practicing control engineers. The guideline offered an accurate assessment of the chattering behaviors, and a catalogs implementable SMC design solutions. It also provided a frame of reference for future SMC researches [35]. Fig. 3.12 shows the effect of chattering on sliding surface. It is continues on-off switching form.

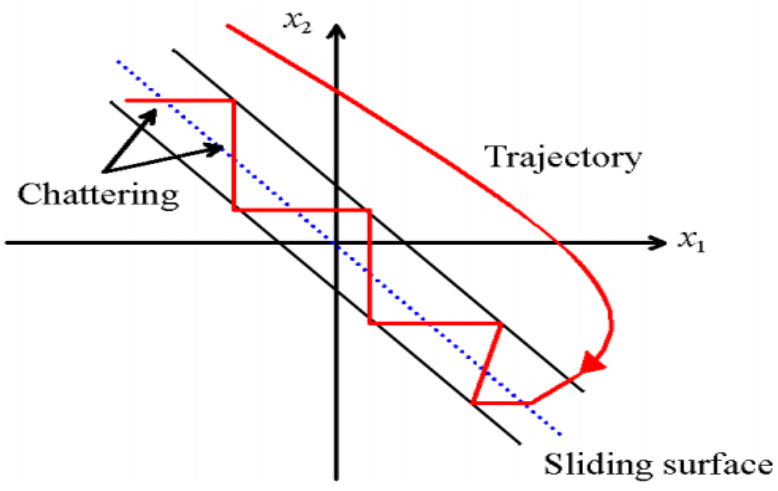

Fig. 3.122: Chattering effect of SMC [35]

To restrain the effect of chattering, saturated function sat(s) shown in Fig. 3.13 is adopted instead of sign(s).

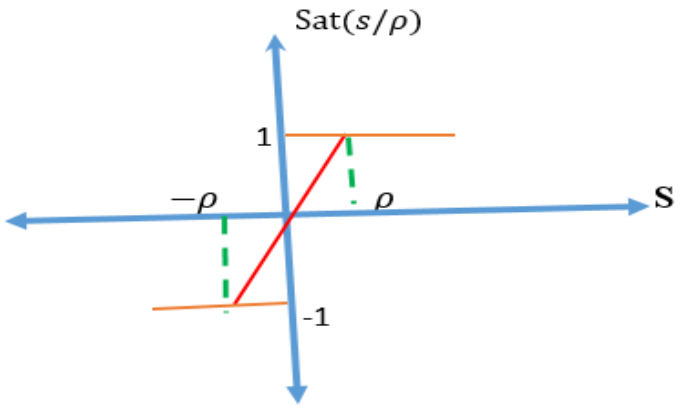

Fig. 3.13: Saturation function [30]

$$sat(s) = \begin{cases} 1, & for\ s > \rho \\ \frac{s}{\rho}, & abs(s) \leq \rho \\ -1, & s < -\rho \end{cases} \tag{3.72}$$

Where ρ is the "boundary layer".

The nature of saturated function is that out of the boundary layer, switch control is selected, in the boundary layer.

The sat(s) is rewrite in terms of signum function as follows:

$$s_i = \lambda_i e + \dot{e}$$

$$sat(s_i) = \begin{cases} sign(s_i), & if\ abs(s_i) > \rho \\ \frac{s_i}{\rho}, & abs(s_i) \leq \rho \end{cases} \tag{3.73}$$

3.2.3. Fuzzy PID Controller

Fuzzy PID controller are designed for rotational (roll, pitch and yaw) dynamics. The desired roll and pitch angular position called attitude, extracted from the position (X and Y) dynamics. The results are highly affected by noise or disturbance. Adding filter is better to avoid these disturbance. In fuzzy PID controller the PID gain is tuning by fuzzy rule. Its advantage is to reduce overshoot and track the reference trajectory with in short time [36].

Initially the PID controller gain k_p, k_i, k_d are calculated from linearized system by tuning online. This is better to estimate the maximum and minimum stable gain value.

The typical PID control law in its standard form is:

$$U(t) = k_p\left(e(t) + \frac{1}{T_i}\int_0^t e(t)\,dt + T_d\frac{de(t)}{dt}\right)$$

$$U(t) = k_p e(t) + k_i\int_0^t e(t)\,dt + k_d\frac{de(t)}{dt} \qquad (3.74)$$

Where $k_d = k_p * T_d$ and $k_i = k_p / T_i$

$e(t)$ is the difference between desired value and actual value, $U(t)$ control variable, k_p proportional gain, T_d is derivative time constant, T_i the integral time constant, k_d is derivative gain, and k_i the integral gain.

Quadrotor has nonlinear characteristics, while classical control methods like PID are not enough for stabilize and control. Whereas, fuzzy system control is nonlinear and it is thus suitable for nonlinear system control. The fuzzy system can be used for tuning the PID gain parameters [37]. The success of the PID controller based on an appropriate choice of its gains.

3.2.3.1. Fuzzy System for Tuning the PID Gains

The performance of the PID controller based on the appropriate tuning of its gains. PID gain tuning is not a trivial task to optimize performance. In practice, the gains are usually tuned by experienced human experts based on some "rule of thumb". In the work fuzzy IF-THEN rules are used and combined these rules into a fuzzy system that is used to adjust the PID gains on-line [37].

Fig. 3.14 shows that the fuzzy system takes two inputs (e and Δe) and it gives three outputs (k_p', k_i', k_d'). These block diagram just shows control of one degree of freedom of a quadrotor. By using the same method two other controllers are designed for attitude (phi and theta) and heading (psi) control of quadrotor.

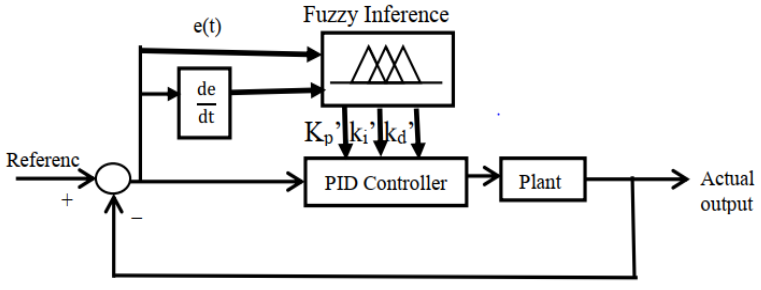

Fig. 3.14: Basic structure of fuzzy PID controller with plant [38]

The Fuzzy-PID controller has relatively smaller errors than the PID controller and has a better capability to reject disturbances in case of attitude controller [38].

The "If-Then" logic can be applied to decrease the position error value on output in the form of quadcopter movement. "Mamdani-type" inference is used for the inference engine with "centroid defuzzification" method, it is more recommended for nonlinear system [37]. The fuzzy PID controller ($U_{fPID}(t)$) is given by:

$$U_{fPID}(t) = k_{pf}\, e(t) + k_{if} \int_0^t e(t)\, dt + k_{df}\, \frac{de(t)}{dt} \qquad (3.75)$$

Where k_{pf} , k_{df} and k_{if} are fuzzy PID controller gain for proportional, integral and derivative, respectively. Initially, the PID gain can be calculated from linearized system using online tuner on Matlab/Simulink. The stability range of gain are obtained are for each gain.

The self-tuning fuzzy PID controller, which takes error "e" and rate of change-in-error "Δe" as the input to makes the controller use of the fuzzy controller rules to update its gains k_p, k_i, k_d online as shown Fig. 3.15. Finding the fuzzy relationship between the three gains of PID controller and "e" and "Δe", and according to the principle of fuzzy control modifying the three gains in order to meet different requirements for control gains when "e" and "Δe" are different and making the control performance is better.

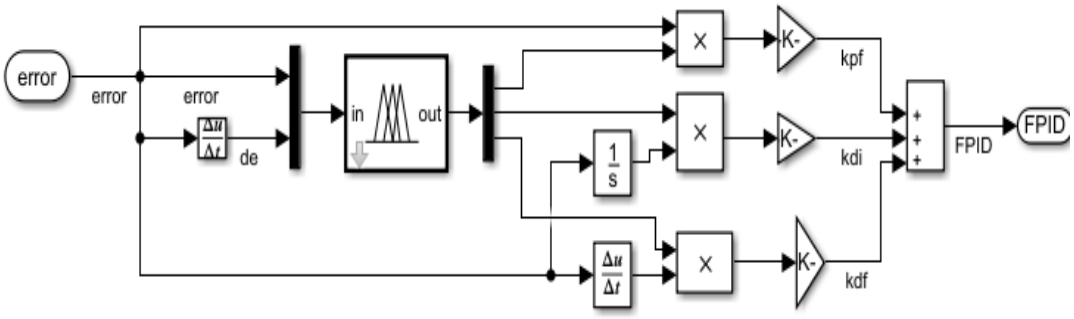

Fig. 3.15: Simulink block diagram of a fuzzy self-tuning PID controller

Fig. 3.16 shows the structure of fuzzy control system, the output tune the appropriate value of PID gain. Mamdani-type fuzzy inference method is the process of formulating the mapping from a given input to an output using fuzzy logic. It is the most commonly seen fuzzy methodology. The output membership functions is fuzzy sets, after the aggregation process, there is a fuzzy set for each output variable that needs defuzzification.

Sugeno-type inference systems can be used to model any inference system in which the output membership functions are either linear or constant [39].

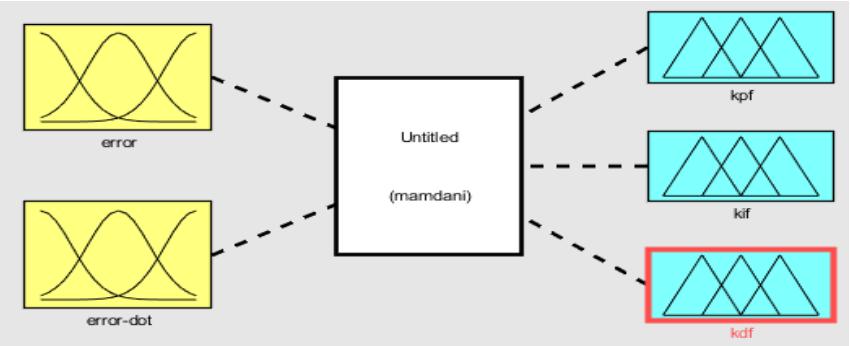

Fig. 3.16: Basic structure of a fuzzy controller

The selected language variables of "e" and "Δe" is choose seven fuzzy values (NB, NM, NS, Z, PS, PM, PB) which denotes Negative Big, Negative Medium, Negative Small, Zero, Positive Small, Positive Medium and Positive Big respectively, and for the outputs we are chosen three fuzzy values (N, Z, P) which denotes, Small, Medium and Big respectively.

The membership functions of the all inputs and outputs have been choice identical. Fig. 3.17 shows structure this membership functions. Because of it covers a wide range of tuning width Gaussian membership functions can be chosen. The range of the fuzzy sets used for controllers are not identical. It is determined by tuning linearized system and taking rang of stability of the linear system or it can be obtained the by using trial and error experience [36].

The range of the fuzzy set for inputs, error and error rate have been chosen [-1 - 1] and for output k_p have been chosen between [0 - 20], k_i have been chosen [0 - 1] and for k_d have been chosen [0 - 8] for attitude (phi and theta) dynamics. The range of k_p have been selected [0 - 25], k_i have been selected [0 - 1] and k_d have been selected [0 - 8] for heading (psi) dynamics.

Fig. 3.17 shows the function range of the error and error rate membership plot, Fig. 3.18a, shows the membership plot of range k_p' for roll and pitch, Fig. 3.18b, shows the membership plot of range of k_i' for roll, pitch and yaw, Fig. 3.18c, shows the membership plot of range of k_d' for roll, pitch and yaw, and Fig. 3.18d, shows the membership plot of range of k_p' for yaw controller.

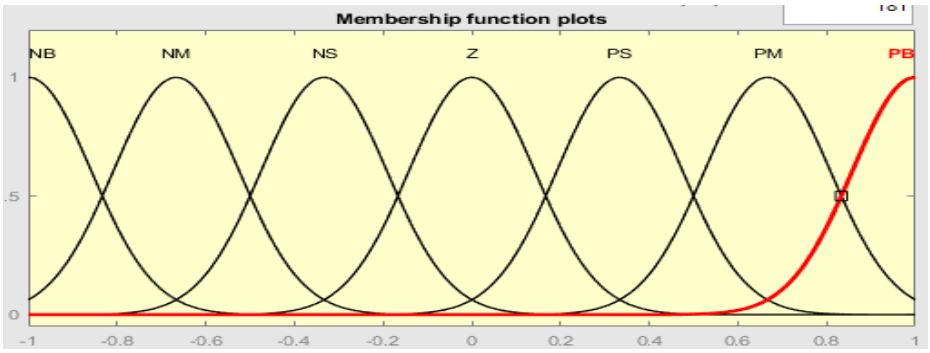

Fig. 3.17: Membership function plot for e and Δe range

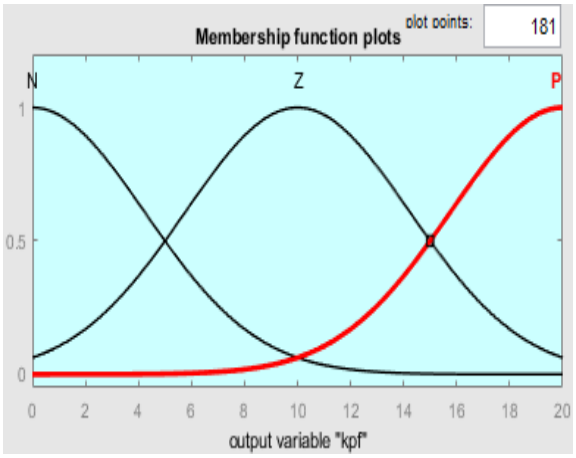

a) Range of k_p' for roll and pitch

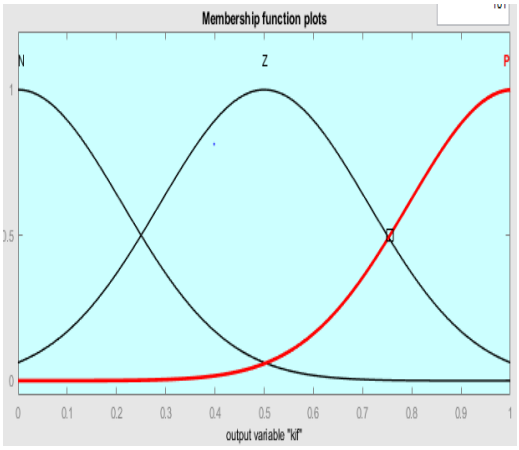

c) Range of k_i' for roll, pitch and yaw

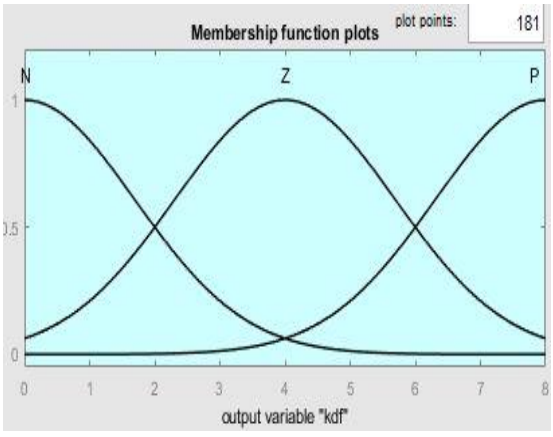

b) Range of k_d' for roll, pitch and yaw

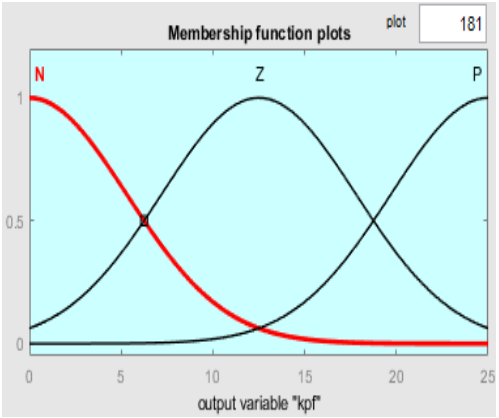

d) Range of k_p' for yaw controller

Fig. 3.18: Range of fuzzy controller gain for the dynamics roll, pitch and yaw controller

Table 3.2 illustrates fuzzy interfacing rule for the rotational (roll, pitch and yaw) dynamics. It has 49 rules.

Table 3.2: Fuzzy interfacing rule for rotational dynamics

e(t)/Δe(t)	NB	NM	NS	Z	PS	PM	PB
NB	N	N	N	N	N	N	Z
NM	N	N	N	N	N	Z	P
NS	N	N	N	N	Z	P	P
Z	N	N	N	Z	P	P	P
PS	N	N	Z	P	P	P	P
PM	N	Z	P	P	P	P	P
PB	Z	P	P	P	P	P	P

This fuzzy rule is identical for all controller types. The relation between fuzzy system and PID controller which is called fuzzy PID controller output gain is calculated from its range of fuzzy controller gain [39].

$$U_{fPID}(t) = k_{pf}\, e(t) + k_{if} \int_0^t e(t)\, dt + k_{df}\, \frac{de(t)}{dt} \tag{3.76}$$

$$\begin{cases} k_{pf} = k_p'(kp_{max} - kp_{min}); \\ k_{df} = k_i'(ki_{max} - ki_{min}); \\ k_{if} = k_d'(kd_{max} - kd_{min}); \end{cases} \tag{3.77}$$

Where k_p', k_i' and k_d' are tuning constant for proportional, integral and derivative gain respectively and its best value were obtained using try and error method.

Chapter Four

Simulation Results and Analysis

In this section, the performance and stability of the proposed control strategy is investigated with and without disturbance. The strategies are simulated using Matlab/Simulink software. In the simulation, the desired or reference trajectory for the quadrotor is chosen randomly in order to check the tracking ability of the proposed control strategies.

4.1. Simulink Block Diagram of the Control System

Fig. 4.1 illustrates the Simulink block diagram of the overall system. It contains altitude (Z-dynamics) control (Fig. 4.2), X-position control (Fig. 4.3), Y-position control (Fig. 4.4), heading yaw controller (Fig. 4.5), attitude roll control (Fig. 4.6) and attitude pitch control (Fig. 4.7) Simulink blocks.

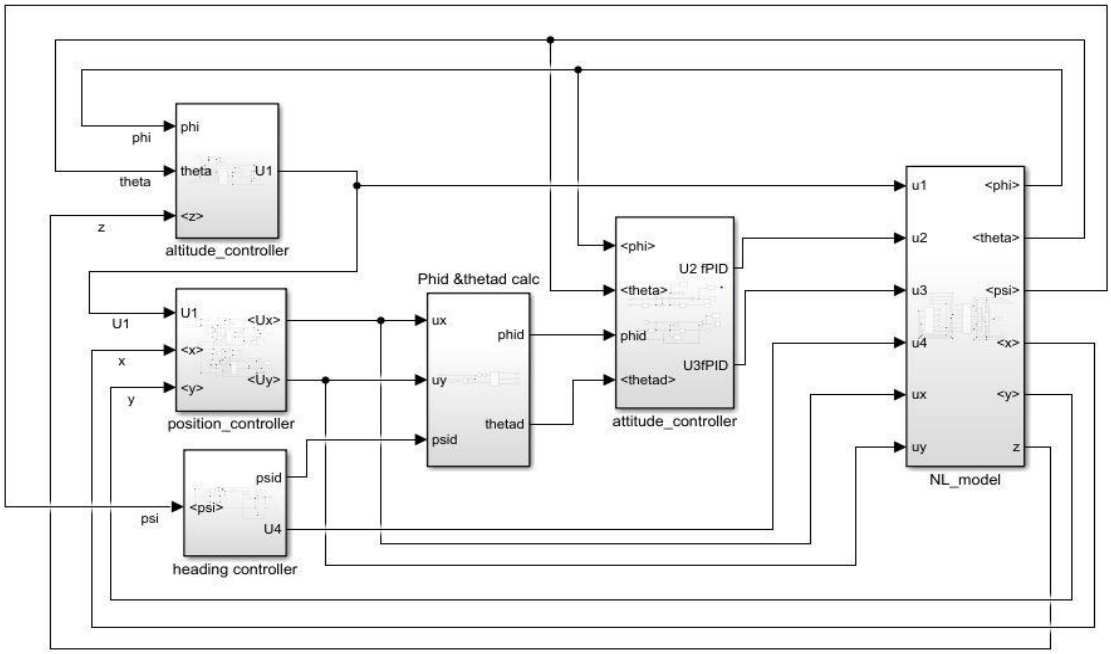

Fig. 4.1: Simulink block diagram of the overall proposed control system

The overall control system, Fig. 4.1, contains the altitude, position, attitude, and heading control sub-system. The position sub-systems contains X and Y control system and the attitude sub-system contains roll and pitch control system.

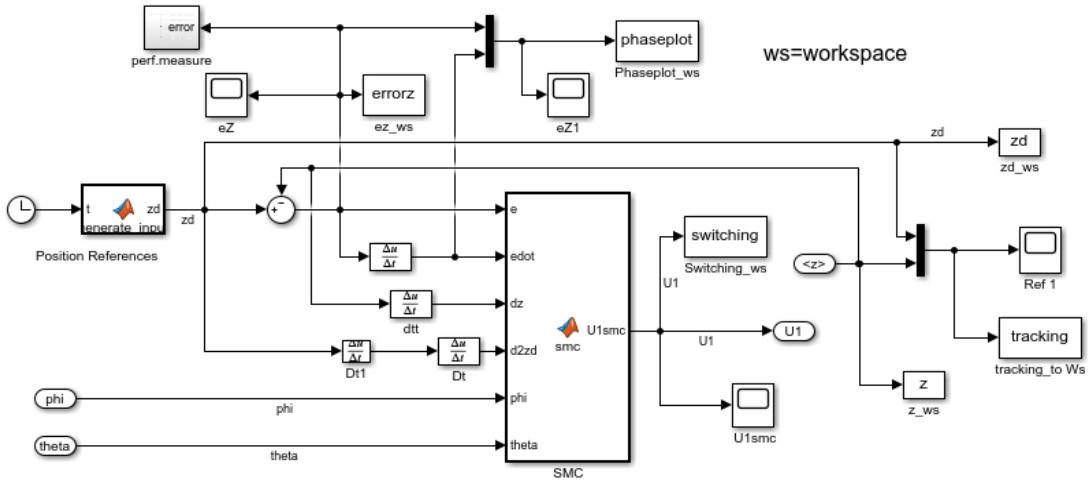

Fig. 4.2: Simulink block diagram of altitude controller

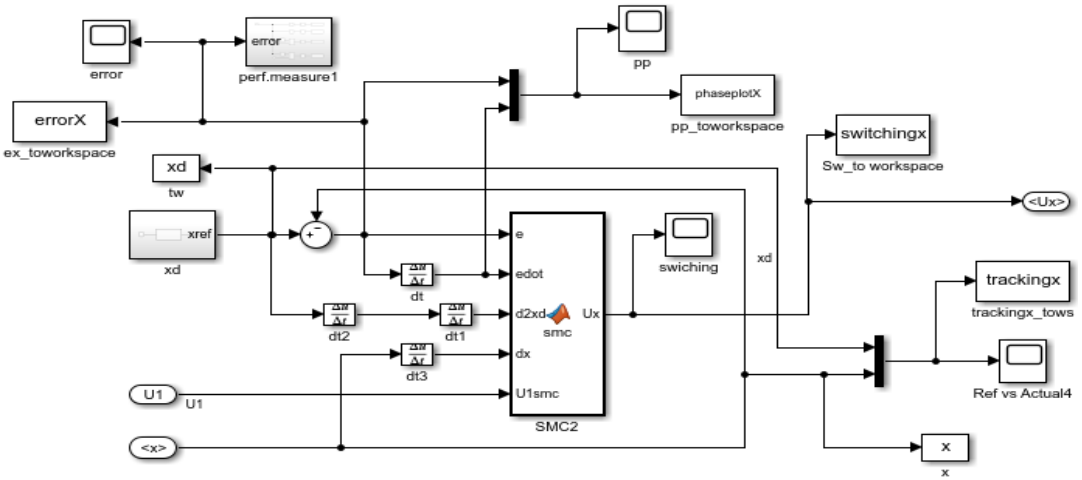

Fig. 4.3: Simulink block diagram for X-position controller

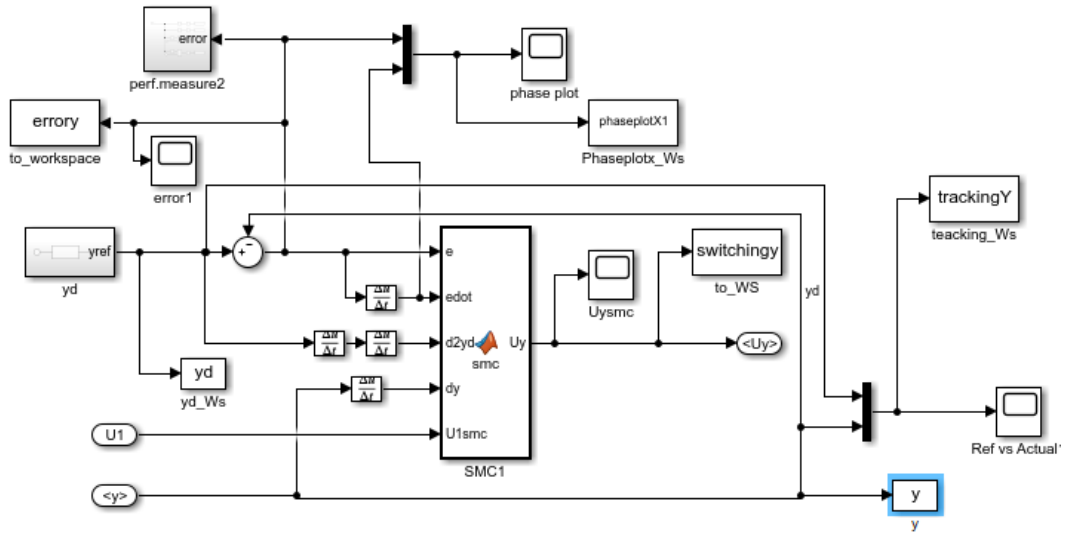

Fig. 4.4: Simulink block diagram for Y-position controller

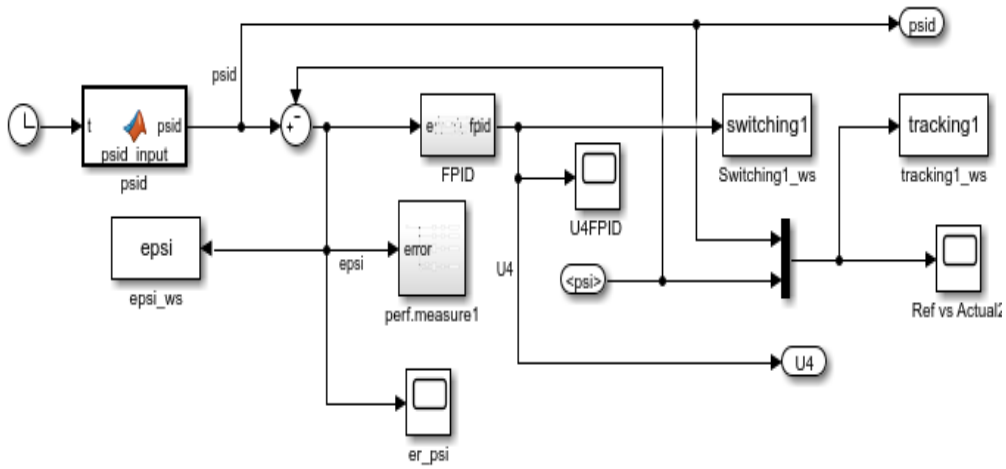

Fig. 4.5: Simulink block diagram of heading yaw controller

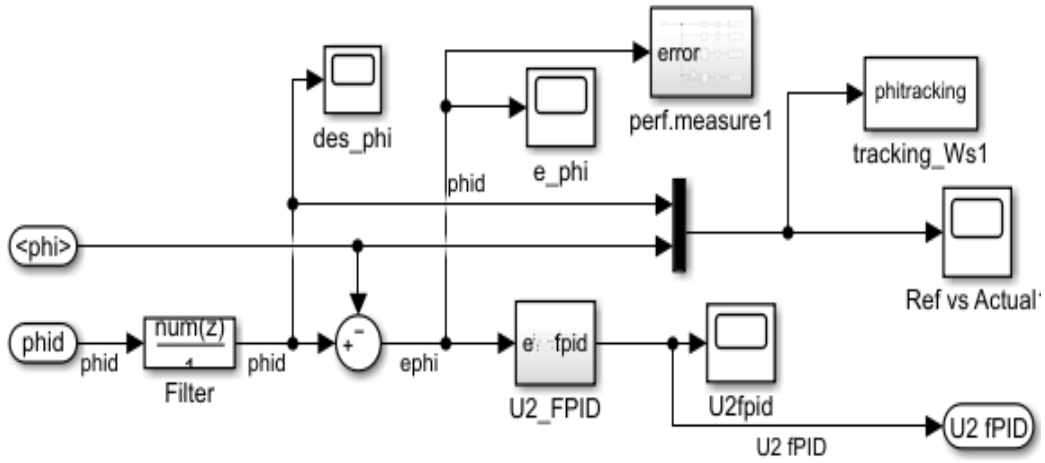

Fig. 4.6: Simulink block diagram of attitude roll controller

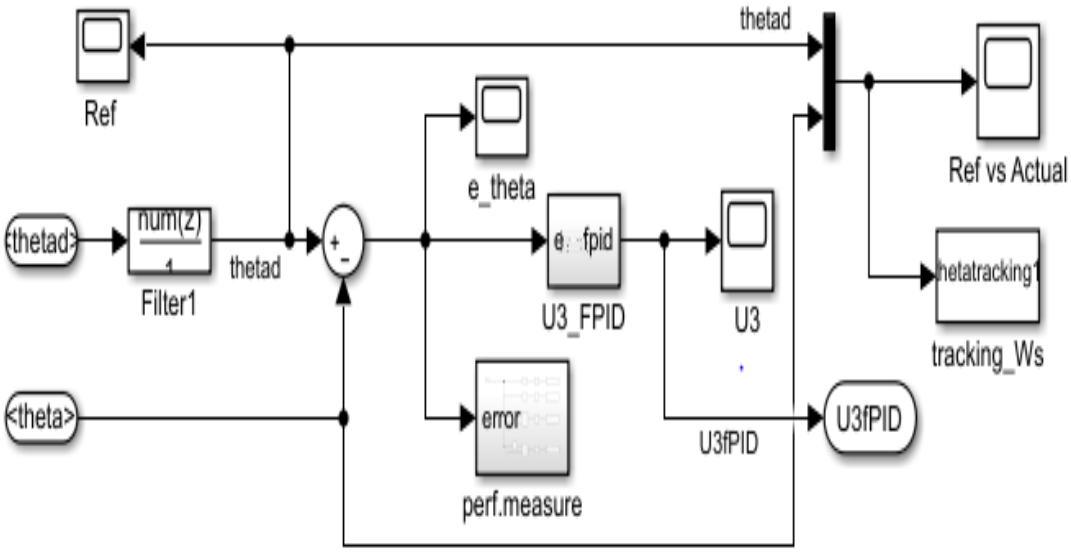

Fig. 4.7: Simulink block diagram for attitude pitch controller

4.2. Parameters Used for Simulation Purpose

Table 4.1: SMC gain parameters used for simulation purpose

Dynamics/state	**K_i for SMC best fit constant**	**λ_i for SMC**	**ρ (boundary layer)**	**Disturbance range**
Roll (phi-attitude)	225	25	0.001	-0.08 to 0.08
Pitch (theta-attitude)	225	25	0.001	-0.08 to 0.08
Yaw (psi-heading)	222	15	0.001	-1 to 1
X (position)	335	15	0.001	-0.45 to 0.45
Y (position)	335	15	0.001	-0.45 to 0.45
Z (altitude)	225	15	0.001	-0.6 to 0.6

Table 4.1 illustrates, SMC constant rate (K_i) and sliding surface coefficient rate (λ_i) for all quadrotor dynamics. There is no general rule in for chosen the gain of SMC. But K_i is greater than 0 in order to satisfy Lyapunov condition in equation (3.4), and λ_i must be Hurwitz. The best fit value are obtained by trial and error approaches.

4.3. Simulation Results of Sliding Mode-Fuzzy PID Control System

In this section the tracking performance of the proposed SM-fuzzy PID control system is tested using different reference trajectories as shown in equation $(4.1a, 4.1b,$ $4.1c, and\ 4.1d)$ below. As described in equation (2.31), the aerodynamic drag force and in equation (2.36), aerodynamic drag torque and gyroscopic torques are incorporated in the nonlinear quadrotor model.

$$\begin{cases} x_d = 4 \cdot \sin(t) \quad m & (4.1a) \\ y_d = 5 \cdot \cos(t) \quad m & (4.1b) \\ z_d = 2 + t \quad\ \ m & (4.1c) \\ \psi_d = 3 \cdot \sin(t) \quad rad & (4.1d) \end{cases}$$

Where $x_d, y_d, z_d,$ and ψ_d are chosen as the desired trajectory for X, Y, Z, and ψ axis, respectively, for simulation purposes.

Initially, the quadrotor is assumed to be on the ground, i.e., starting its flight from altitude and position of [0; 0; 0] m and attitude and heading of [0; 0; 0] rad and follow the desired trajectories. The whole system is simulated for 10 seconds except 3D-helical trajectories.

4.3.1. The Altitude SMC Tracking Performance

It is assumed that the quadrotor starts its flight from ground or zero reference so that altitude is positive. Thus, one can use equation (4.1c) as desired reference trajectory for altitude control. Fig. 4.8 and 4.9 show the tracking performance of the altitude controller for the reference trajectory in equation (4.1c) and the tracking error, respectively. As can be seen from Fig. 4.8, the reference trajectory starts from 2m after 0.3 second the actual path tracks the reference one and after 0.4 seconds, the tracking error becomes very small around 0.001 shown Fig 4.9. This implies that the quadrotor asymptotically follows the desired altitude trajectory with acceptable error.

Fig. 4.10a illustrates the phase portrait plot. From the plot it can be seen that the system reaches the sliding surface with less than 0.4 seconds. This demonstrates the SMC altitude control system is stable. Fig. 4.10b shows the altitude control input (U1) in (N).

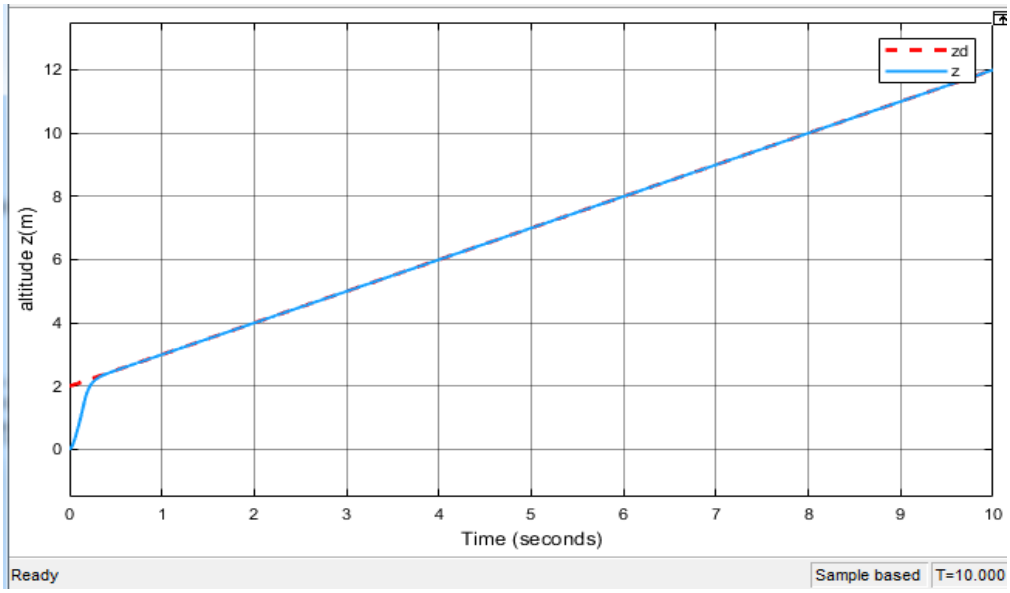

Fig. 4.8: Altitude reference trajectory tracking controller performance using SMC

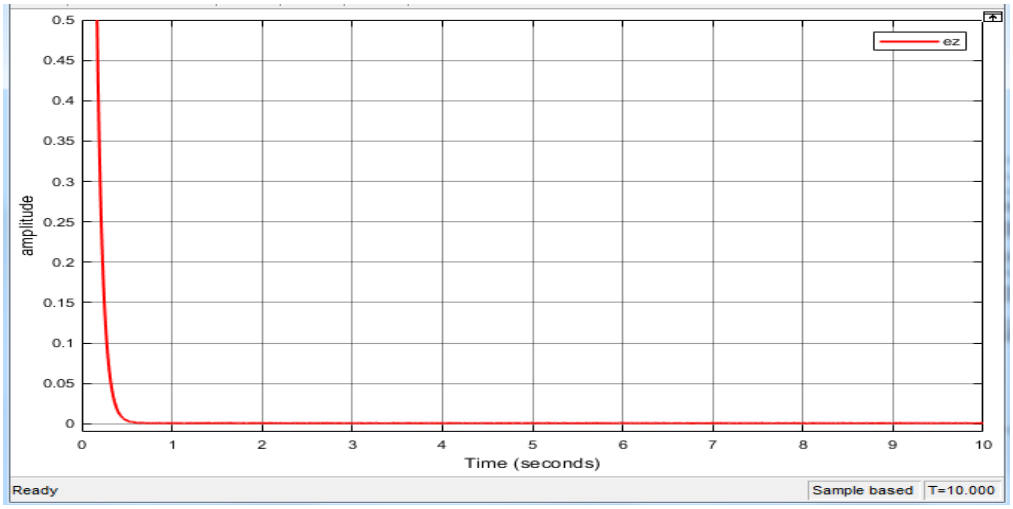

Fig. 4.9: Altitude reference tracking error

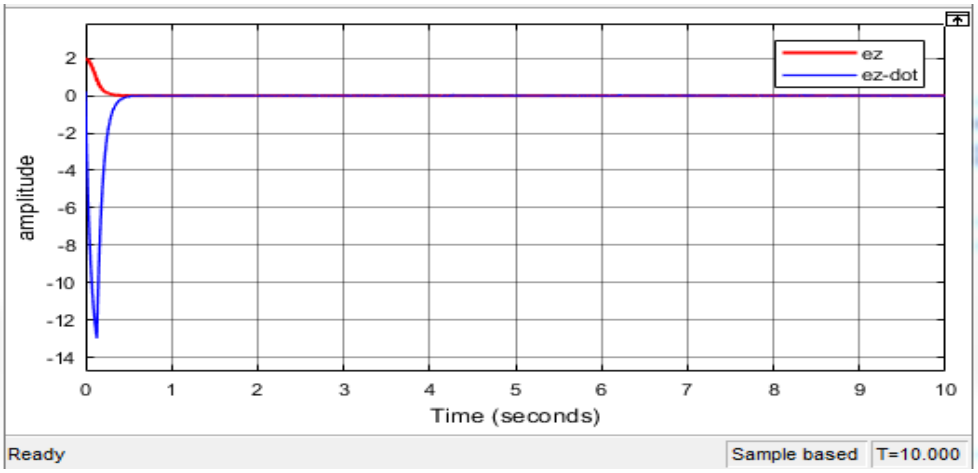

a) Phase portrait plot

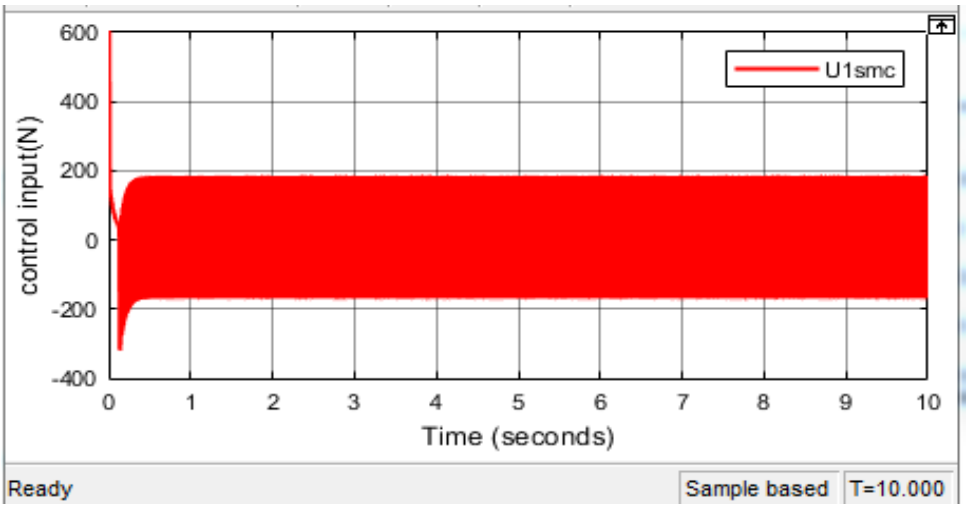

b) Altitude control input

Fig. 4.10: Altitude z-dynamics a) Phase portrait plot b) Control input

4.3.2. Position X and Y Dynamics SMC Tracking Performance

The position control system is the external loop control in the quadrotor control system. It is used to extract the desired attitude roll and pitch positions. The effect of roll and pitch dynamics on the overall system dynamics are described in equation (2.44). It shows that the interaction between position and attitude dynamics.

Fig. 4.11 and 4.12 show tracking performance of SMC to track the in the X and Y positions at a given reference trajectories as shown in equation $(4.1a)$ and $(4.1b)$, respectively. The actual path (x) track the given trajectory ($x_d = 4.\sin(t)$) at 0 second. In case of Y position the actual trajectory the desired ($y_d = 5.\cos(t)$) one, after 0.4 seconds, it is because of desired path (y_d) is start from (x=0 and y=5) and the actual path (y) is start from the origin. The result demonstrates that the proposed controller have achieved its tracking objectives in both positions.

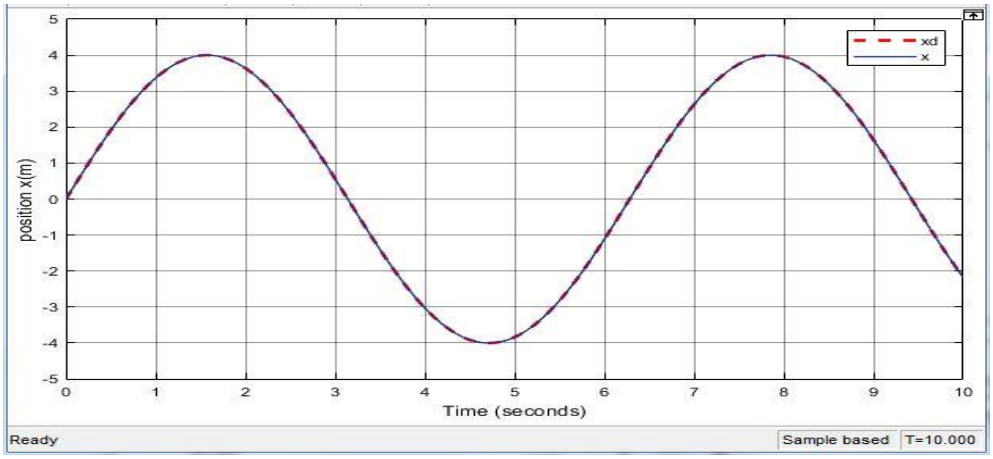

Fig. 4.11: Trajectory tracking controller performance of x-position using SMC

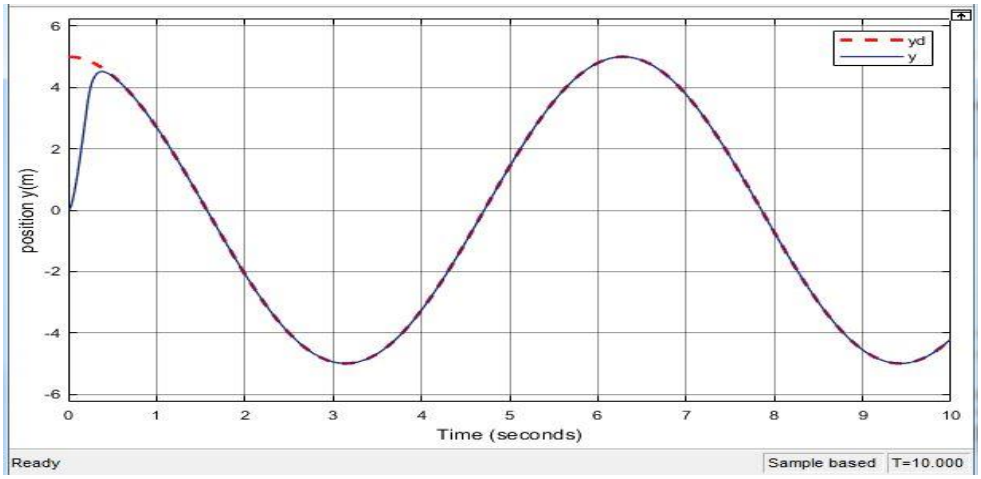

Fig. 4.12: Trajectory tracking control performance of y-position using SMC

Fig. 4.13 and 4.14 show the position tracking errors for x and y dynamics. One can observe that the error for x-dynamics and y-dynamics are within the range of ± 0.05 % and ± 0.1 %, respectively. It means the quadrotor follows the desired position trajectory with a minimum acceptable error.

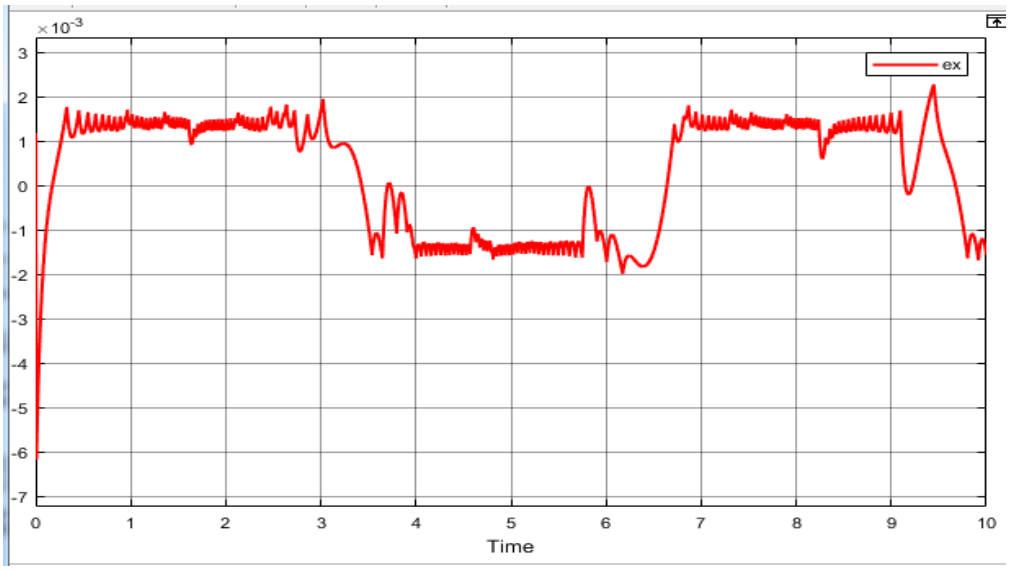

Fig. 4.13: Tracking error of x-position controller

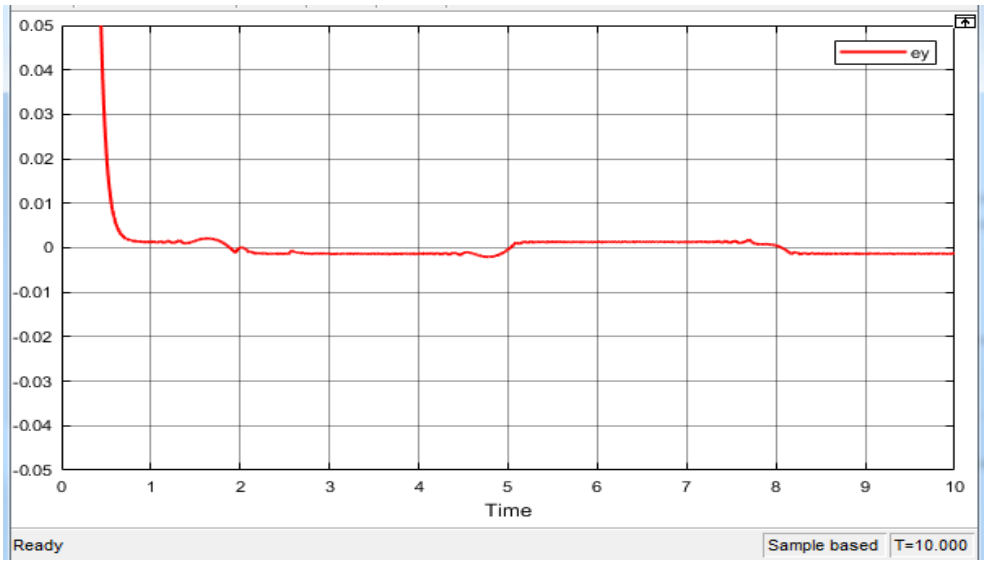

Fig. 4.14: Tracking error of y-position controller

Fig. 4.15 and 4.16 show the phase portrait plot (simply phase plot) of x and y positions, respectively, and obtained by plotting error and its rate. It shows time interval that the actual trajectory reached to desired one, called reaching phase. And also it tells the control system stability and controller efficiency. The actual path reaches the reference trajectory at 0 second for X-trajectory, and 0.4 seconds for Y-trajectory.

From the plots it can be seen that the system reaches the sliding surface with in a very small time interval. This demonstrates that the SMC based position control system is stable.

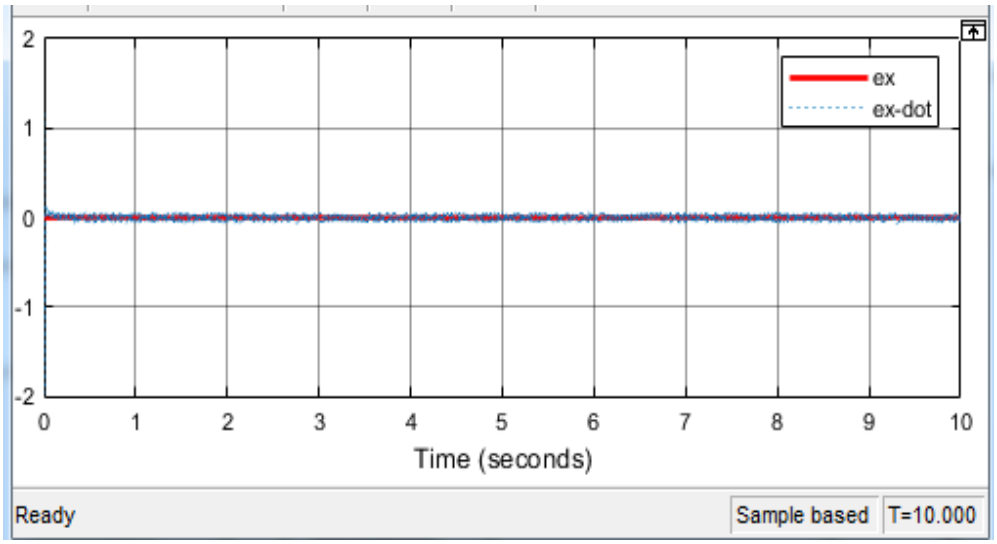

Fig. 4.15: Phase portrait plot of the position x dynamics

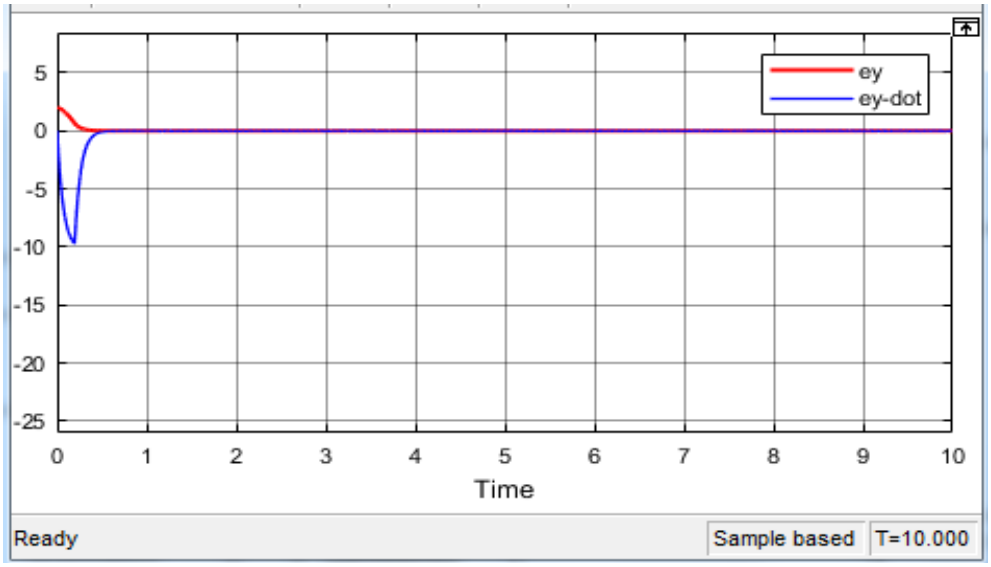

Fig. 4.16: Phase portrait plot of the position y dynamics

4.3.3. Fuzzy PID Attitude Controller Tracking Performance

The dynamic relation between position (X and Y) and attitude (roll and pitch) are highly coupled and nonlinear. As a result, the output extracted from the position dynamics before the desired attitude reached is highly oscillatory and noisy. In order to extract pure attitude trajectory, or to remove noise and disturbance from the trajectory, filtering is used after the output signal or before it reach at of the desired attitude trajectory.

Then, square wave type trajectory is generated and given to the fuzzy PID attitude control, the tracking performance are seen in Fig. 4.17 and 4.18.

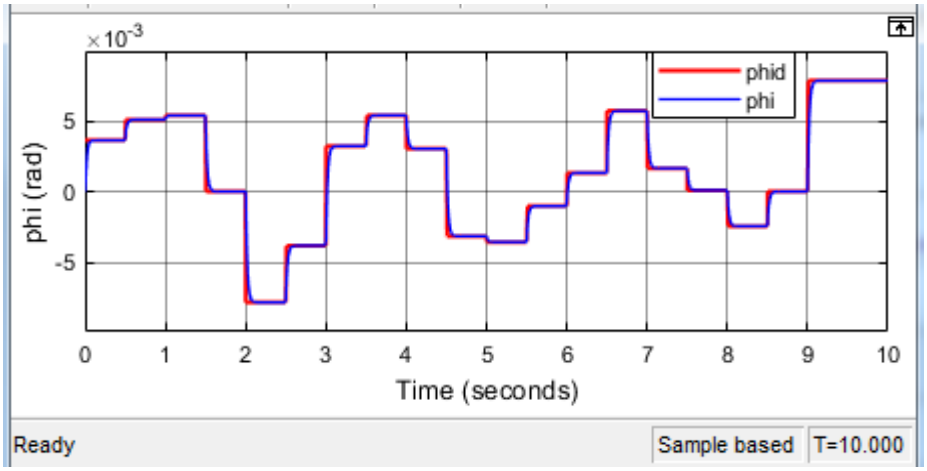

Fig. 4.17: Attitude trajectory tracking result of roll using fuzzy PID controller

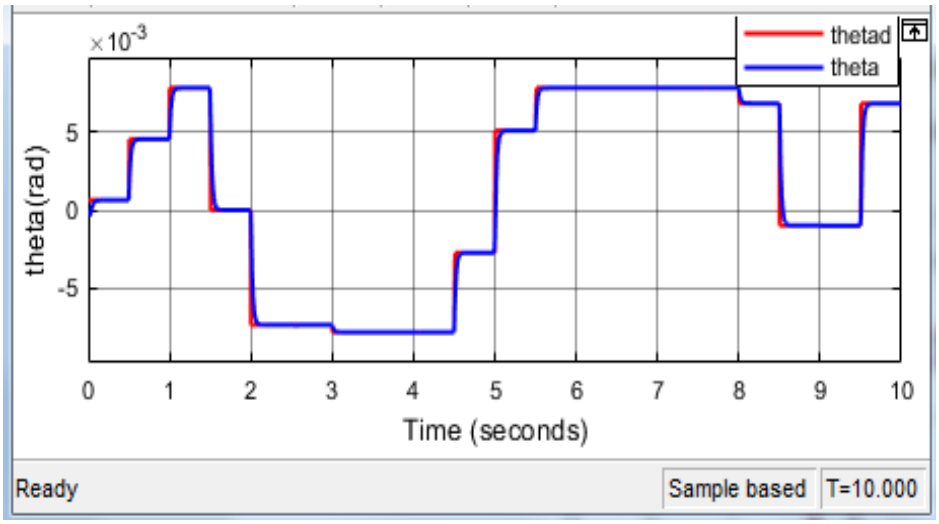

Fig. 4.18: Attitude trajectory tracking result of pitch using fuzzy PID controller

Fig. 4.17 and 4.18 show the reference trajectory tracking performance of attitude roll (phi) and pitch (theta) dynamics using fuzzy PID controller, respectively. The desired trajectory were bounded in between [$^{-\pi}/_{2}$ to $^{\pi}/_{2}$ rad] in order to avoid singularity of the system as described in equation (2.2). Even though the reference trajectories were changed in every moment, the proposed control scheme managed to effectively hold the quadrotor's attitude in finite-time as shown Fig. 4.17 and 4.18. The results demonstrate that the proposed fuzzy PID controller have achieved its tracking objectives in both cases.

Fig. 4.19 and 4.20 show fuzzy PID attitude roll and pitch controller tracking error, respectively. The tracking error range is $\pm 0.5*10^{-3}$ except at the edge of the trajectory. At the edge of the square wave trajectory the controller takes a new action to track the trajectory as a new reference. The results tell that the controller action are very fast to forcibly attract the actual output to the reference trajectory.

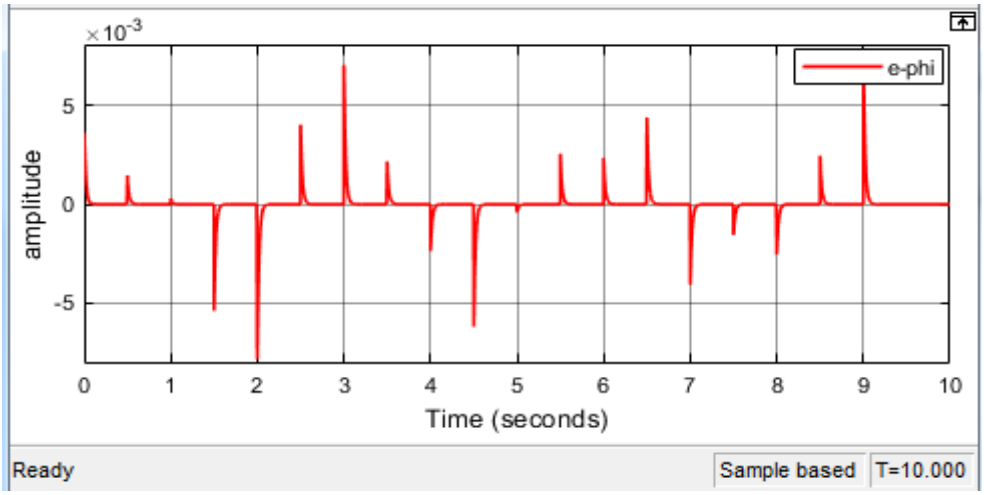

Fig. 4.19: Attitude tracking error of roll trajectory

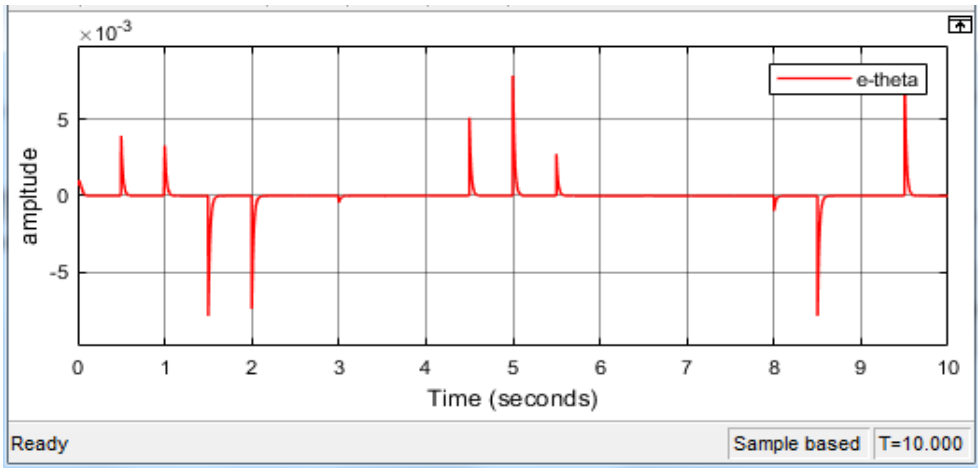

Fig. 4.20: Attitude tracking error of pitch trajectory

Fig. 4.21a and 4.21b are the control input signals of the attitude roll and pitch dynamics, respectively. This control input signals are the roll and pitch torque as defined in equation (2.24).

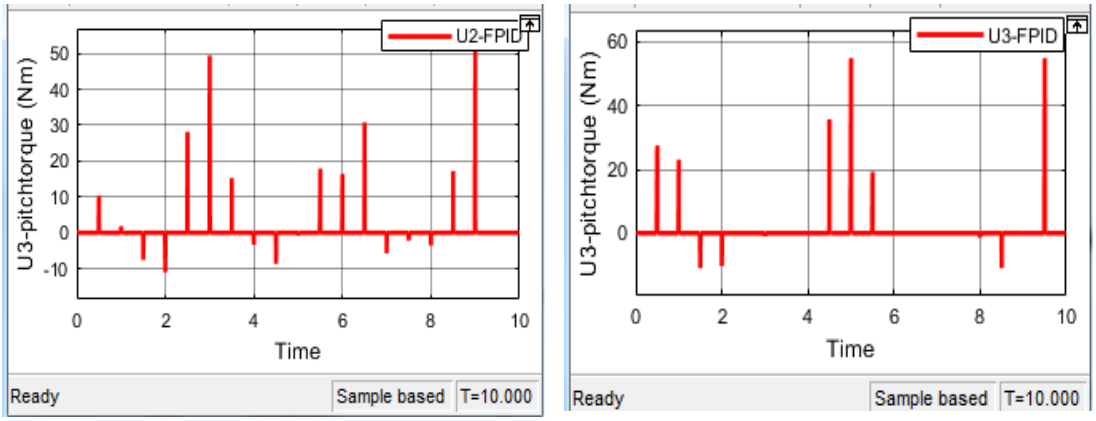

a) Fuzzy PID Control input for roll b) Fuzzy PID Control input for roll

Fig. 4.21: Fuzzy PID control input for attitude a) roll b) pitch dynamics

4.3.4. Fuzzy PID Heading Controller Tracking Performance

The yaw or heading controller is used as a direction controller and guider for the quadrotor. Therefore, the controller must have a better and fast control action as seen in Fig. 4.22. The actual output starts from the origin while the desired one starts from point (x=0 and y=3). From the result the actual trajectory track the desired path defined in equation (4.1d) before 0.2 seconds. Its tracking error is around ± 0.00002 as shown Fig. 4.23. So that, the proposed fuzzy PID controller gave a very good transient responses. The time required for tracking the desired trajectory is very small. This implies that the control action is very fast and with acceptable error.

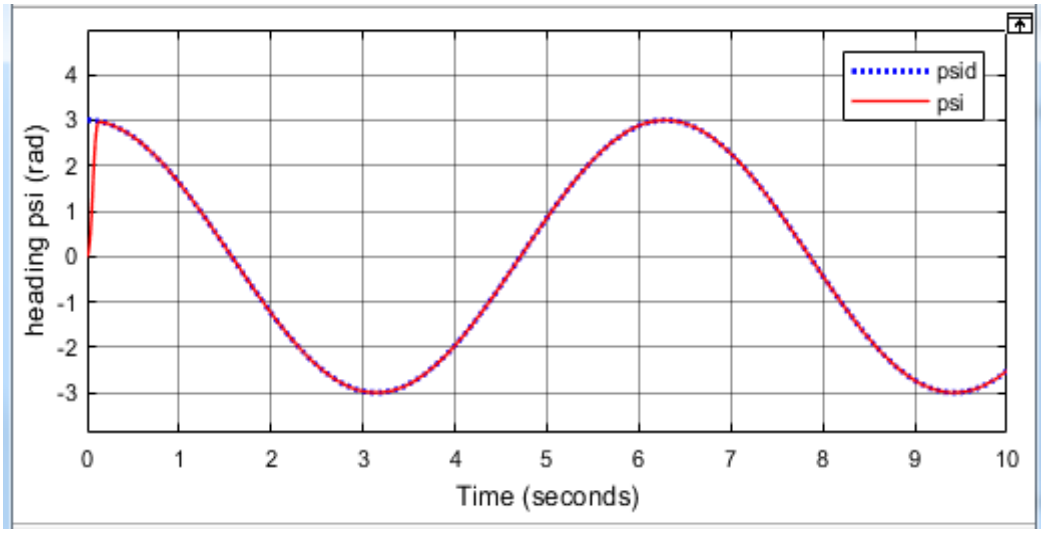

Fig. 4.22: Trajectory tracking performance of heading dynamics fuzzy PID controller

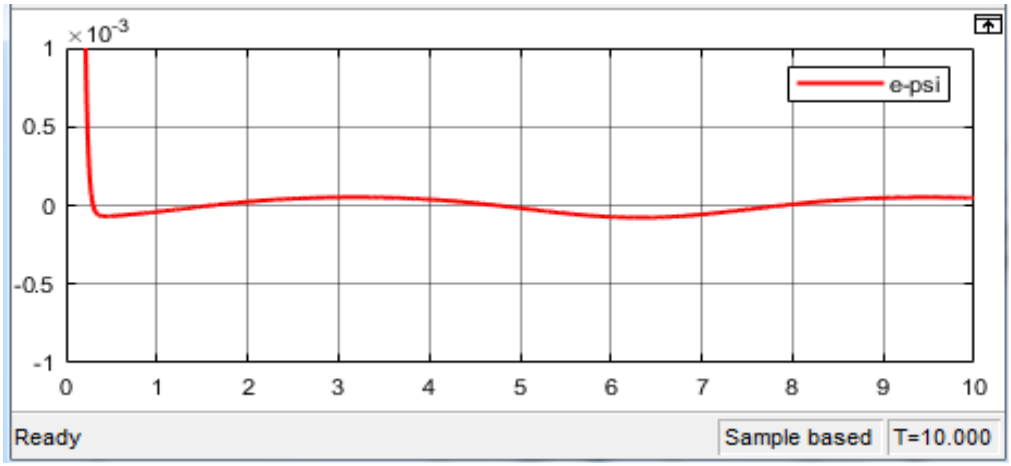

Fig. 4.23: Tracking error of heading (yaw) trajectory using fuzzy PID controller

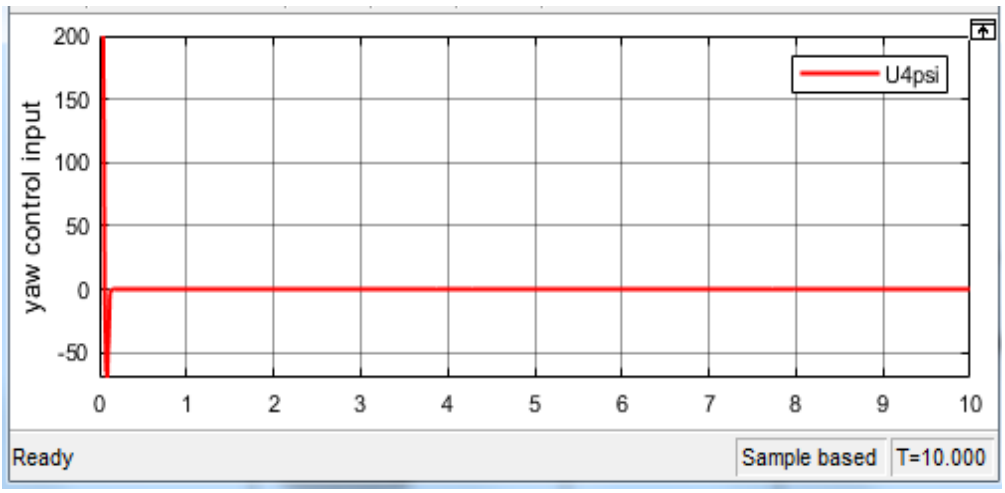

Fig. 4.24: Fuzzy PID control input for heading controller

Fig. 4.22 and 4.23 show the heading trajectory tracking performance and it's tracking error, respectively. As defined in the range of yaw (psi) positions in equation (3.2) it is between [-π upto π rad]. Fig. 4.24 shows the control input signal for heading dynamics, this is called yaw torque as described in equation (3.24).

4.3.5. 3D-Helical Trajectory Tracking Performance

In this subsection SMC approaches for 3D-helical trajectory tracking controller were applied for translational (X, Y, and Z) dynamics in space. It can be seen that from Fig. 4.25 and Fig. 4.26, a better 3D-helical path tracking has been achieved. Fig. 4.25 shows 3D-helical reference trajectory which is generated when the quadrotor is flying initially from point (0, 0, 0) m following the trajectories (5t, 5cos (t), t) m in the X, Y, and Z directions, respectively.

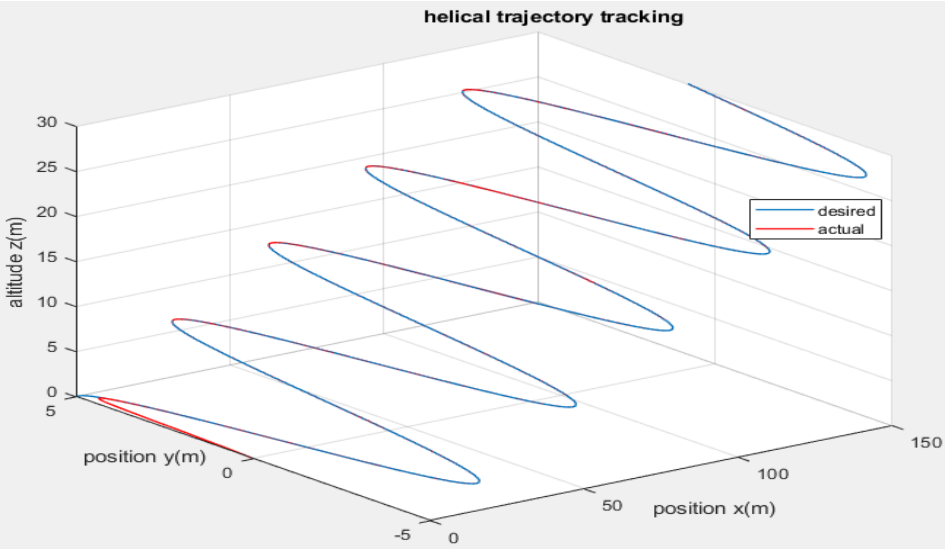

Fig. 4.25: SMC 3D-helical trajectory tracking for (5t, 5cos (t), t) m

Fig. 4.26 demonstrate the tracking performance of the quadrotor while following helical trajectory. The trajectory is generated starting from (0, 0, 0) position following (4sin (t), 5cos (t), 2+t) m trajectories in the X, Y, and Z positions, respectively.

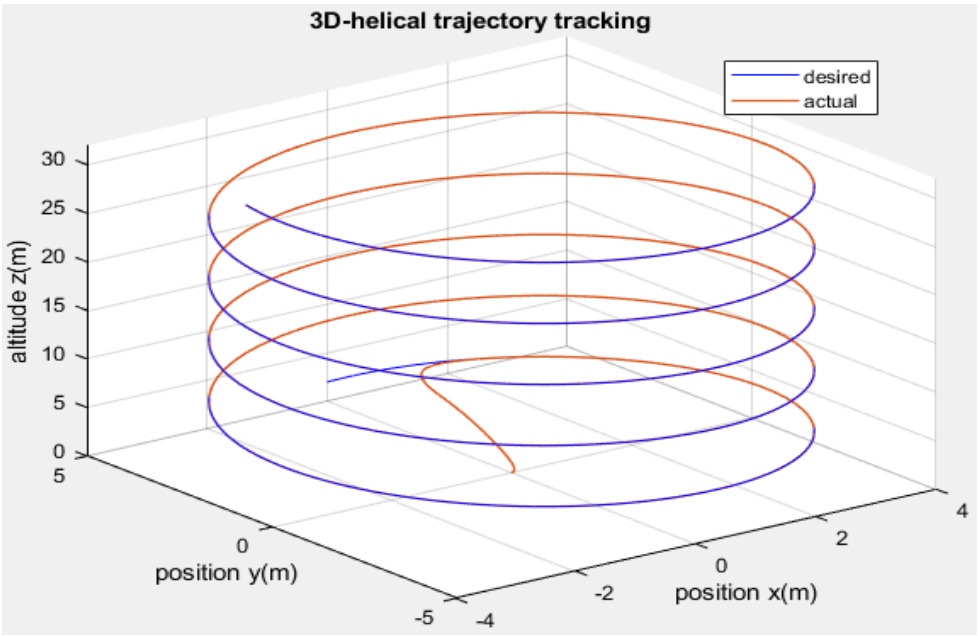

Fig. 4.26: SMC 3D-helical trajectory tracking for (4sin (t), 5cos (t), 2+t) m

The 3D-helical trajectory tracking are shows that the controller performance and its robustness.

4.4. Simulation Result of the Proposed Control System with Disturbance

In this section the proposed (sliding mode-fuzzy PID) controller performance is tested in the presence of random disturbances as shown in Fig. 4.27. It shows the output of a random disturbance signal with uniform or Gaussian (normal) distribution. The type disturbance specifically includes air variation, wind and rain effects, which are appear in real system of quadrotor. The same type of disturbance were added to position (X and Y) and for attitude (roll and pitch) at specific range illiterates in Table 4.1.

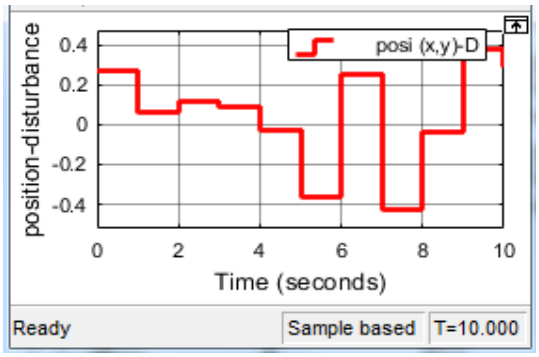

a) Position disturbance

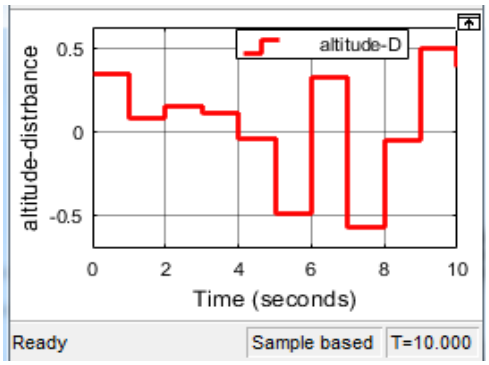

c) Altitude disturbance

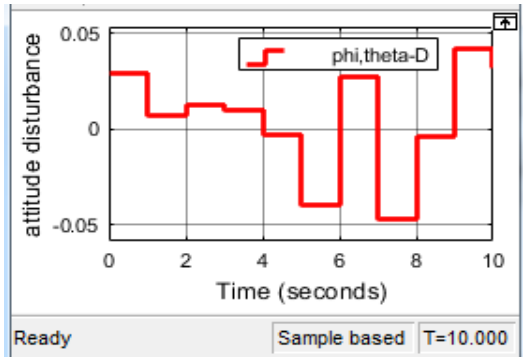

b) Attitude disturbance

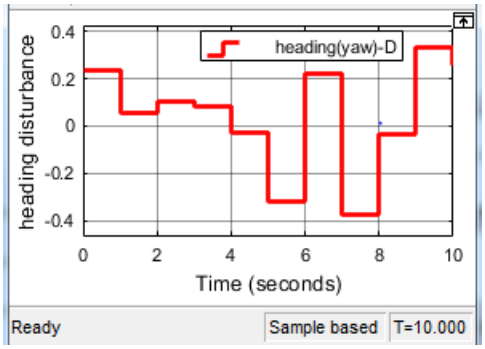

d) Heading (yaw) disturbance

Fig. 4.27: External random disturbance of position, altitude, attitude and heading dynamics

Fig. 4.28 demonstrates the proposed control strategies tracking performance of the altitude, position and heading dynamics while adding the external random disturbance of quadrotor positions. SMC is used for altitude and position (X and Y) and Fuzzy PID controller is used for heading control. The desired trajectories are the same as defined in equation $(4.1a, 4.1b, 4.1c, 4.1d)$ for X, Y, Z, and ψ dynamics.

Fig. 4.29 shows the tracking efficiency of the proposed fuzzy PID controller for attitude (roll and pitch) control.

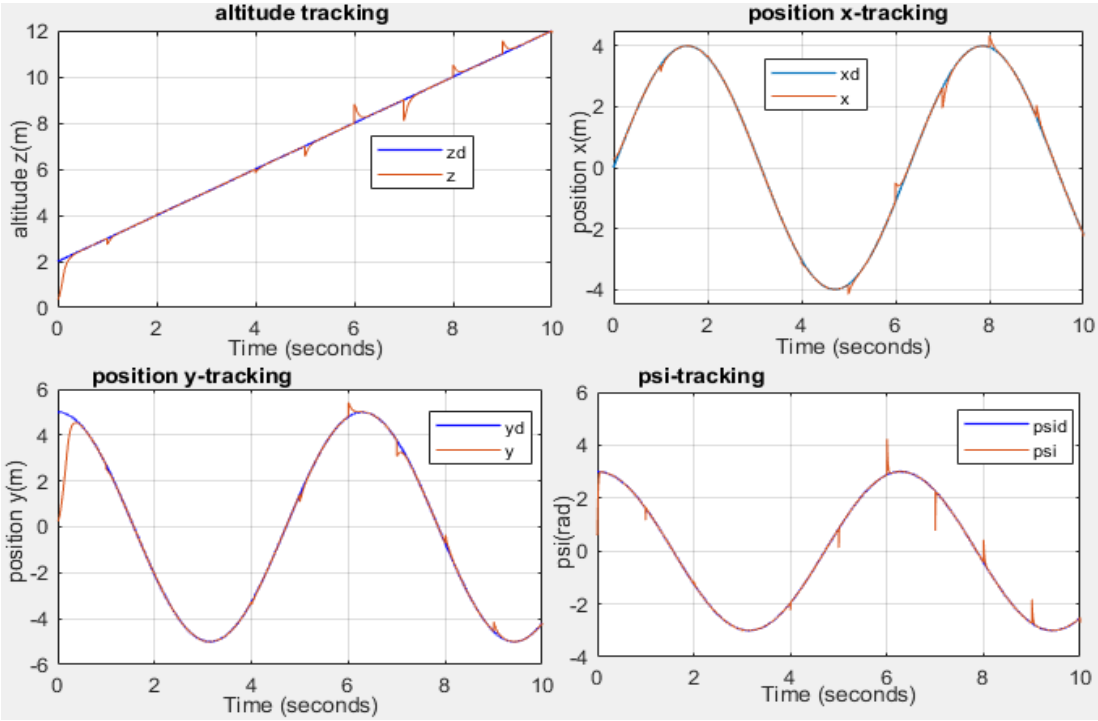

Fig. 4.28: Trajectory tracking control performance of the altitude, position and heading controller with external disturbance added on the system

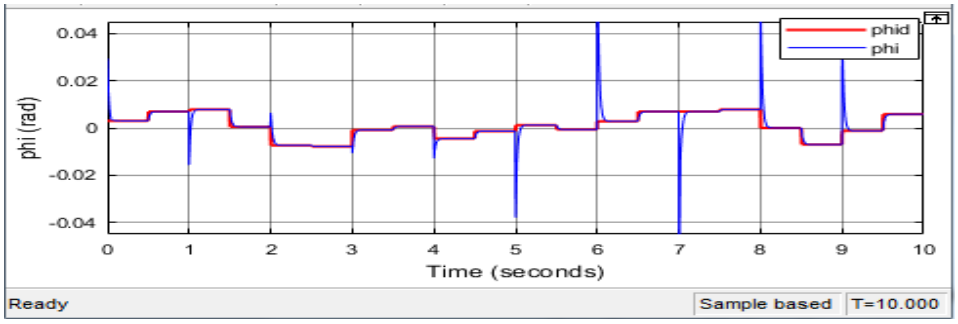

a) Roll attitude (phi) trajectory tracking with disturbance

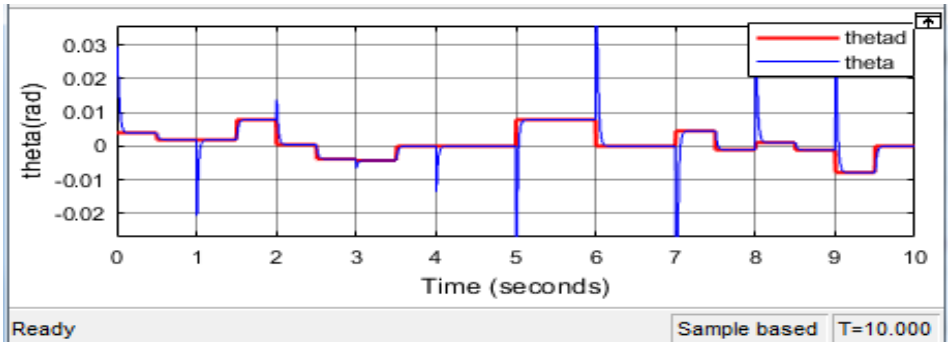

b) Pitch attitude (theta) trajectory tracking with disturbance

Fig. 4.29: Trajectory tracking control performance of the attitude controller with external disturbance added on the system

The results show that when the unknown disturbance is suddenly added on the system, the proposed controller automatically take corrective action to fix the system become stable and reject disturbance effects as illustrates in Fig. 4.28 and 4.29. The time required for the controller to correct the effect of disturbance is less than 0.2 second. This shows that the proposed controller is robust in terms of disturbance rejection.

Fig. 4.30 shows the path tracking error of position (X and Y) and altitude (Z) SMC. And, Fig. 4.31 shows the trajectory tracking error of attitude (roll and pitch) and heading (yaw) using fuzzy PID controller with the presence of random external disturbance.

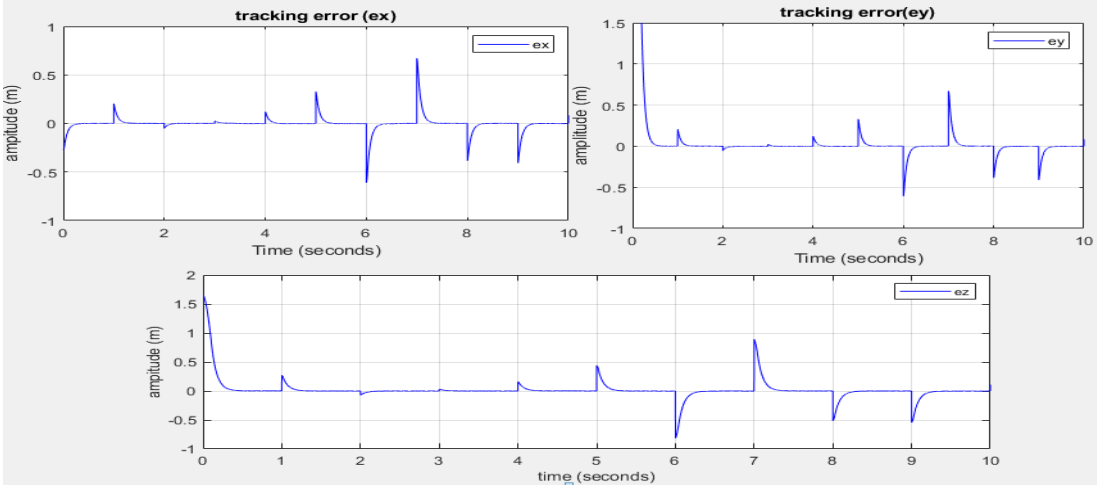

Fig. 4.30: Trajectory tracking error of position and altitude controller with the presence of disturbance

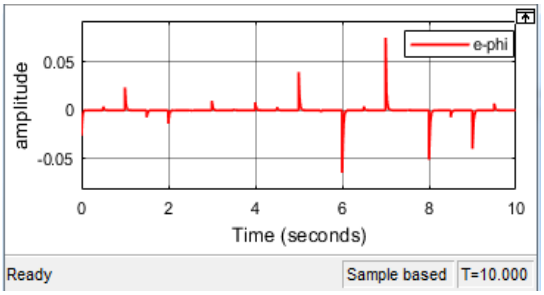

a) Roll tracking error

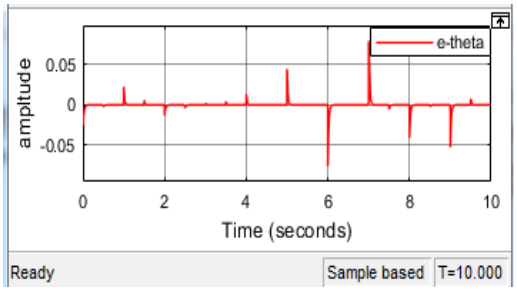

b) Pitch tracking error

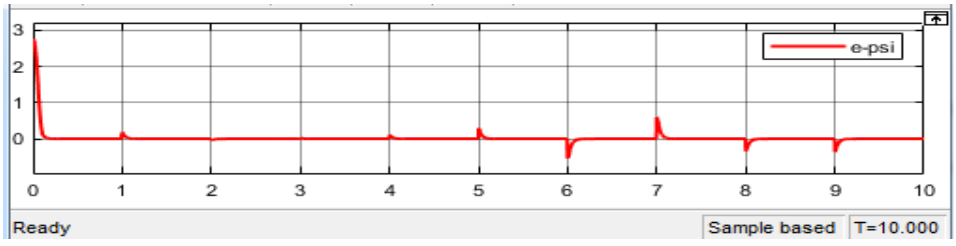

c) Heading tracking error

Fig. 4.31: Trajectory tracking error of roll, pitch and heading with the presence of disturbance

The tracking error results show some chatter property, this results were occurred because of the noise or disturbance we added. The controller corrected the effect of this disturbance within short period of time (around 0.15 seconds for SMC and 0.1 seconds for fuzzy PID controller).

4.5. SMC Simulation Results for Rotational Dynamics

This simulation is done to compare the performance between SMC and Fuzzy PID controller when applying for rotational (roll, pitch, and yaw) dynamics. In the proposed control system, SMC for translational (X, Y, and Z) and fuzzy-PID controller for rotational (roll, Pitch, and yaw) dynamics have designed and simulated in subsection (4.3) and (4.4) without and with presence of external disturbance, respectively.

In this section applying SMC instead of fuzzy-PID controller for rotational (roll, pitch and yaw) dynamic is shown, i.e., the whole system is controlled by SMC. The controller performance are shown in Fig. 4.32 for roll, Fig. 4.33 for pitch and Fig. 4.34 for yaw trajectory tracking.

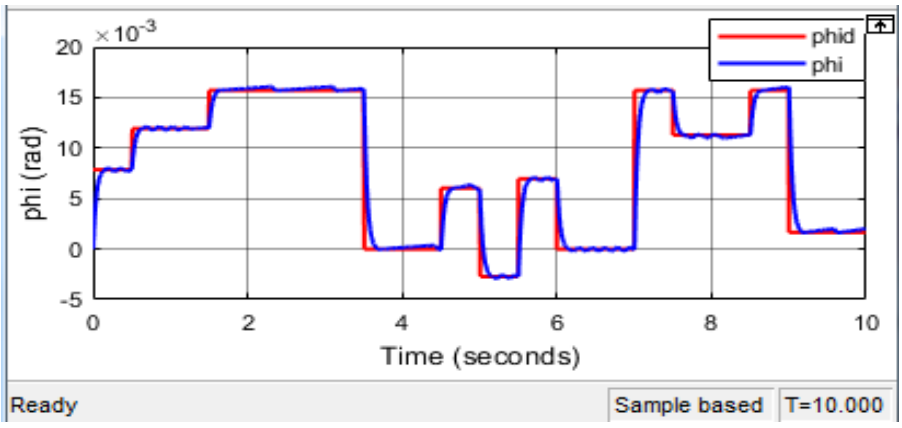

Fig. 4.32: SMC attitude roll-trajectory tracking control performance

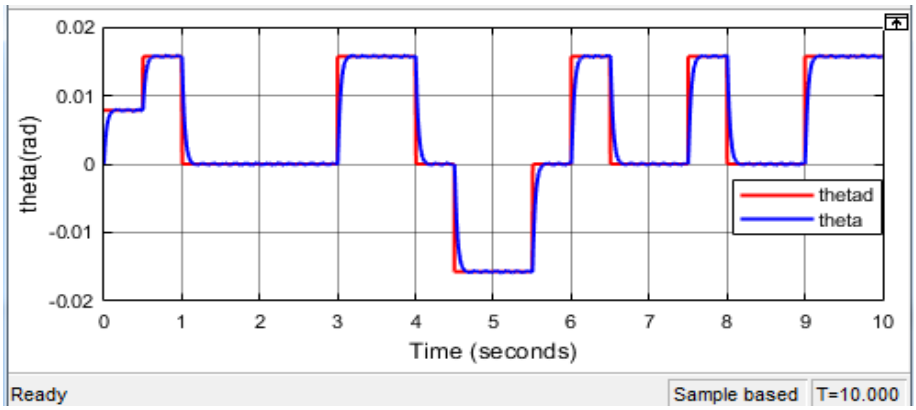

Fig. 4.33: Attitude theta-path tracking control performance of SMC

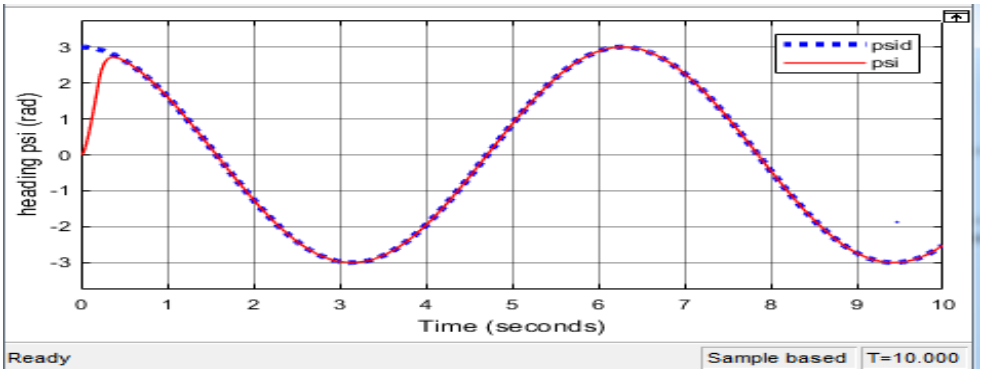

Fig. 4.34: Heading psi-path tracking control performance of SMC

Trajectory tracking error for roll, pitch and yaw are illustrated in Fig. 4.35a, Fig. 4.35b, and Fig. 4.35c, respectively. These results demonstrate the performance of SMC applied to the rotational dynamics.

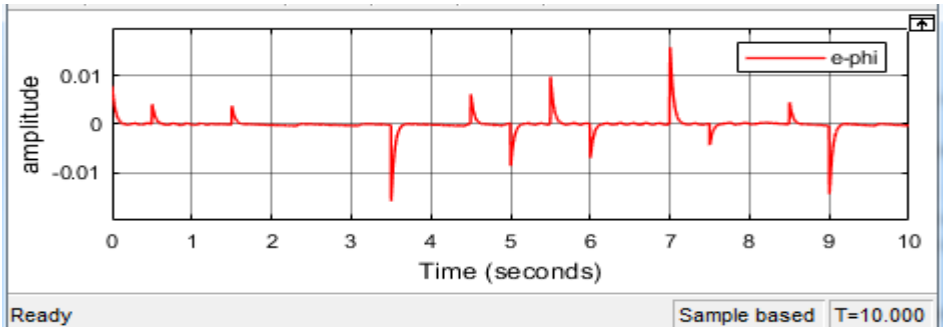

a) Tracking error of attitude phi-trajectory using SMC

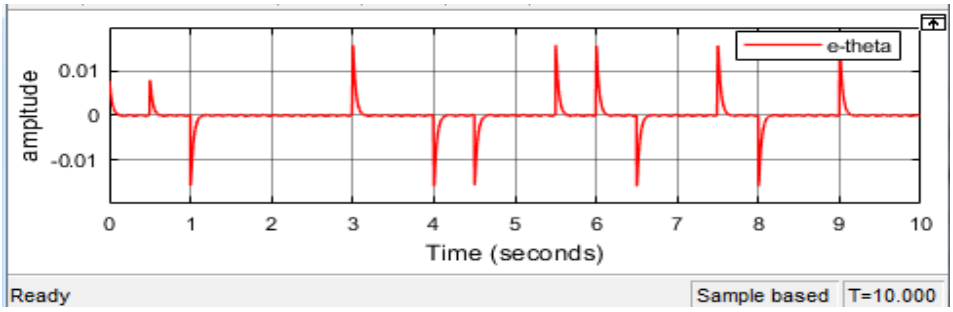

b) Tracking error of attitude theta-trajectory using SMC

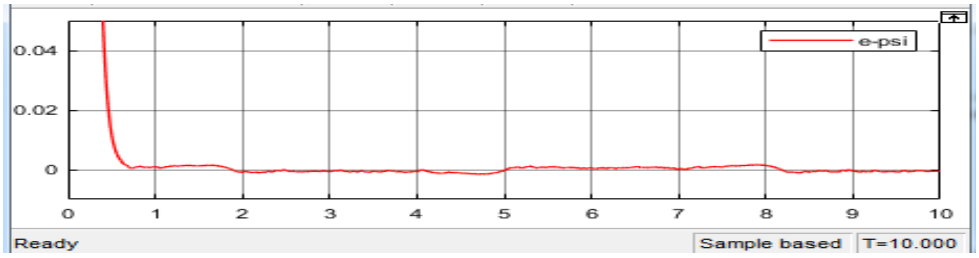

c) Tracking error of heading psi-trajectory using SMC

Fig. 4.35: SMC Trajectory tracking error of a) roll b) pitch c) heading dynamics

Attitude tracking errors in Fig. 4.19 and Fig. 4.20 are obtained by using fuzzy PID controller for roll and pitch, respectively. Whereas, Fig. 4.35a and Fig. 4.35b are done by using SMC controller. The results clearly show that tracking errors of fuzzy-PID controller are smaller than the tracking errors that are obtained from SMC controller. The speed of response time is also faster in case of fuzzy-PID controller than SMC by 0.1 - 0.4 seconds. Similarly for yaw dynamics the tracking error in Fig. 4.23 is obtained by applying fuzzy PID controller and Fig. 4.35c is done by using SMC. The result demonstrates that fuzzy PID controller have better tracking performance than that of SMC for rotational dynamics.

The control input for dynamic model that are assigned in equation (2.24) were the vertical thrust force (U_1), roll torque (U_2), pitch torque (U_3) and yaw torque (U_4). Fig. 4.36a, 4.36b, and 4.36c show the roll, pitch, and yaw torque respectively.

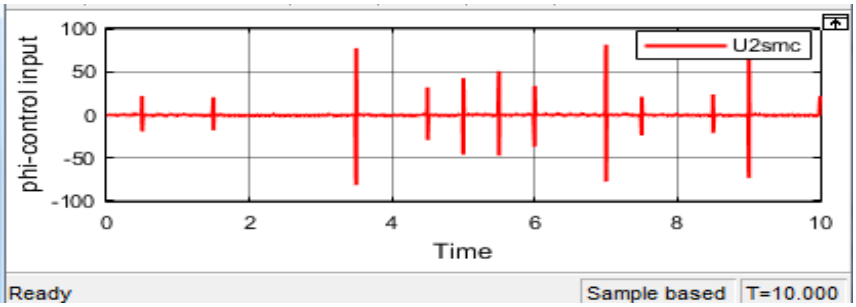

a) SMC control input for phi-attitude dynamics

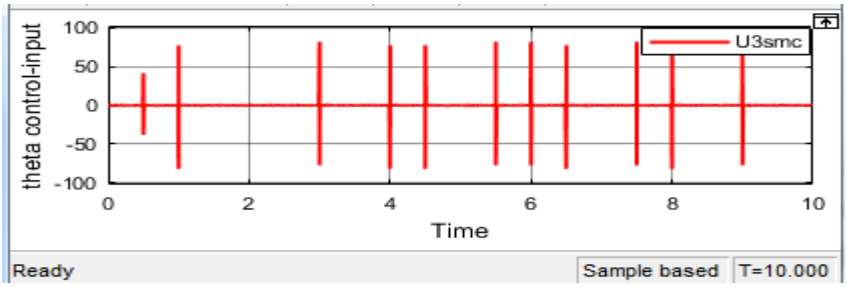

b) SMC control input for theta-attitude dynamics

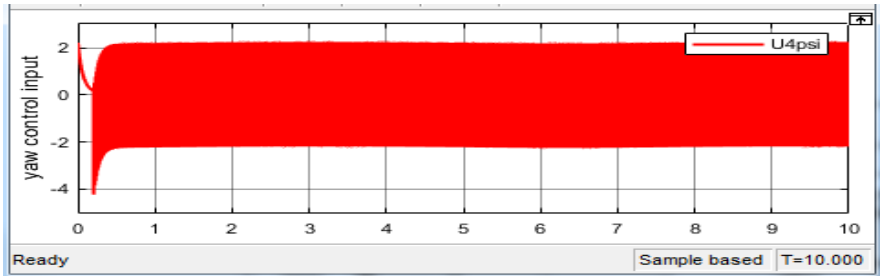

c) SMC control input for psi-heading dynamics

Fig. 4.36: SMC control input for a) roll b) pitch c) yaw dynamics

Phase portrait plot of SMC for rotational roll, pitch and yaw dynamics are shown in Fig. 4.37a, Fig. 4.37b, and Fig. 4.37c, respectively. The system reaches the sliding surface within short time. This demonstrates that the SMC rotational dynamic control system are stable.

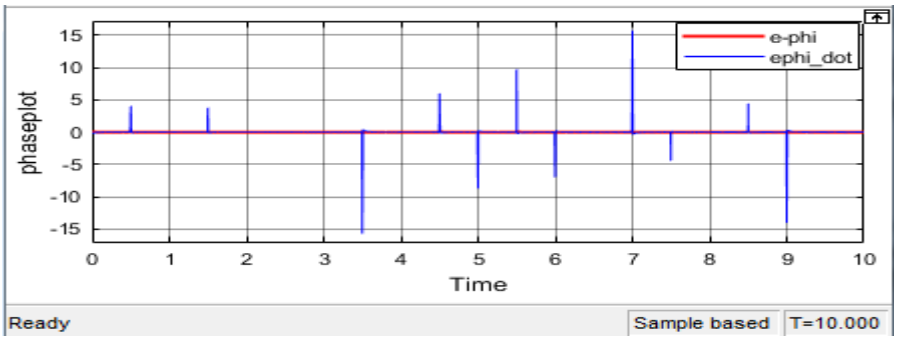

a) Phase plot for attitude phi-controller

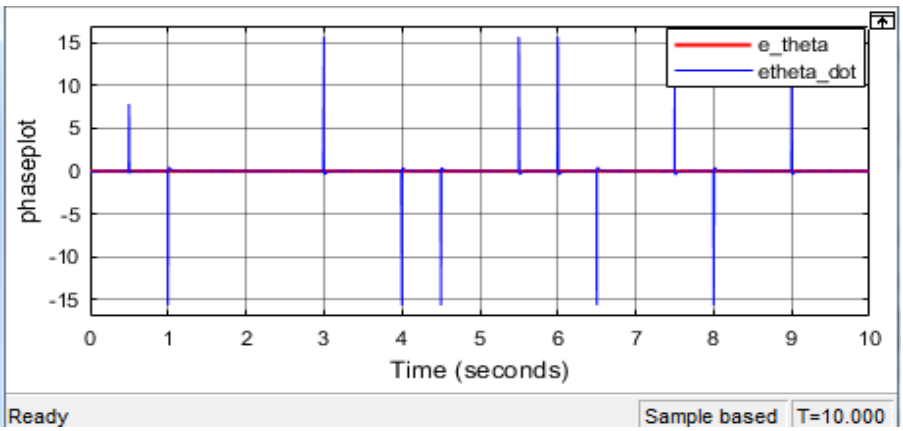

b) Phase plot of attitude theta-controller

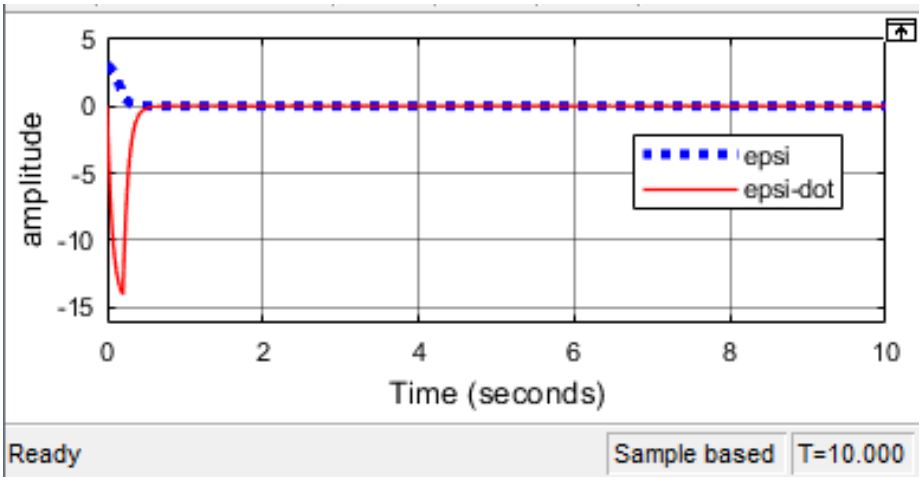

c) Phase plot of heading psi-controller

Fig. 4.37: Phase-plot for a) roll-attitude b) pitch-attitude c) yaw-heading controller

4.6. Comparative Analysis

In this section the performance of rotational dynamic control using SMC and the proposed fuzzy PID controllers are compared. Integral square error (ISE), integral absolute error (IAE), integral time square error (ITSE), and integral time absolute error (ITAE) indices are used as performance measure as listed in appendix A. The results are summarize in the Table 4.2 and 4.3.

Table 4.2: SM - fuzzy PID controller performance indices

State of the dynamic model	**Performance index for SM - FPID controller**			
	ISE	**IAE**	**ITSE**	**ITAE**
Phi/roll	3.454*10^-6	0.001329	1.55*10^-5	0.006053
theta/pitch	3.69*10^-6	0.001133	1.829*10^-5	0.00513
Psi/yaw	0.4223	0.1854	0.01181	0.008821
X	8.438*10^-6	0.005329	1.376*10^-5	0.02348
Y	0.4672	0.336	0.03469	0.06729
Z	0.3693	0.2805	0.02211	0.09636

Table 4.3: SMC performance indices

State of the dynamic model	**Performance index for SMC for all system**			
	ISE	**IAE**	**ITSE**	**ITAE**
Phi/roll	2.539*10^-5	0.005202	0.000145	0.02766
theta/pitch	5.429*10^-5	0.006993	0.0002874	0.03558
Psi/yaw	1.073	0.512	0.08145	0.09059
X	1.798*10^-5	0.01295	8.721*10^-5	0.06423
Y	3.089	0.8813	0.2428	0.1614
Z	0.3796	0.2866	0.02333	0.09409

From the performance index table presented above, SM - fuzzy PID controller has smaller values in all performance measures than SMC. This shows that the proposed fuzzy PID controller demonstrate better path tracking performance for heading control and attitude dynamics. Fig. 4.38 shows the graph of performance indices for roll (ϕ),

pitch (θ), yaw (ψ), position (x), position (y), and for altitude (z) controller obtained based on Table 4.2 and 4.3 values. The ISE at point one (1), IAE at point two (2), ITSE

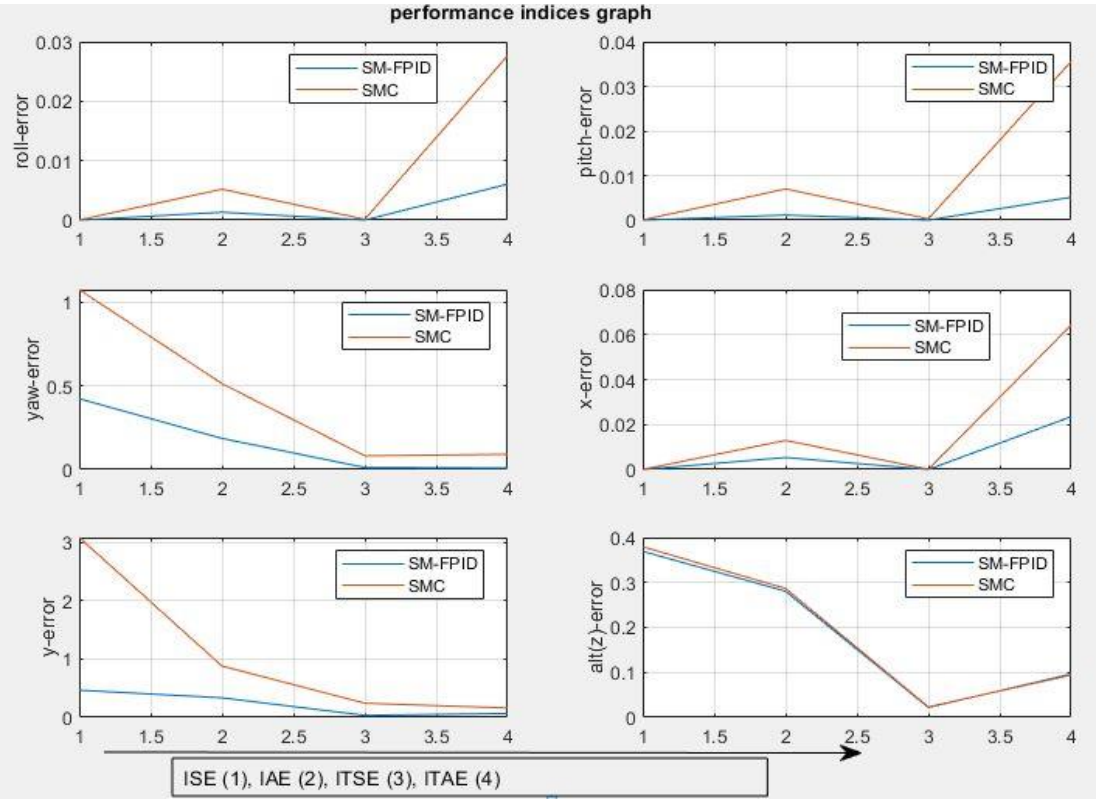

at point three (3), and ITAE at point four (4) in the x-label.

Fig. 4.38: Performance indices graph of SMC and SM-FPID controllers

The performance indices graph and tables shows that smaller error is obtained by SM-FPID than that of SMC. Based on IAE value in Table 4.2 and 4.3, as compared from SMC, SM-FPID controller reduced the error by 74% for roll, 84% for pitch, 64% for yaw, 59% for x, 62% for y, and 2.1 % for altitude.

Chapter Five

Conclusions and Future Works

5.1. Conclusions

In this work the nonlinear dynamic model of quadrotor (quadcopter) are obtained using Newton-Euler formalization. The nonlinear quadrotor model has translational and rotational dynamics (Euler-dynamics). The gyroscopic moment effect resulting from body of quadrotor and rotor blade are considered and aerodynamic drag torque and force incorporated in the model. SM-fuzzy PID controller for the driven nonlinear dynamic were designed.

In order to verify the validity and efficiency of the controller proposed here simulation using Matlab/Simulink was performed. The fuzzy PID controller is used for controlling the rotational dynamics (attitude and heading) of the quadrotor. For translational dynamics (position and altitude) SMC controller is applied. The Fuzzy PID controller has faster transient response than SMC for rotational dynamics.

Translational dynamics (position and altitude) control has three states and are highly coupling-nonlinear, for both input and output states and also the control input. So that, Fuzzy PID controller cannot achieve that. Therefore, SMC is used for these type of systems. Comparison between mixed sliding mode - fuzzy PID controller and SMC alone are done using controller performance indices.

The result shows mixed fuzzy PID and SMC controller reduced the integral absolute error by 57% in average of aver all system. And achieved a better tracking performance than SMC alone. When the quadrotor is flying there are many unknown or unmodeled disturbances affect its motion and the stability of the quadrotor. In order to check the controller robustness by guessing unmodeled external disturbance with in some range and it is added to the output state of the quadrotor. The proposed SM-PID controller managed this effect of disturbance effectively. That means the controller automatically adjust (take a fast action) and make a stable track. Therefore, the designed control system is robust in terms of disturbance rejection.

In the case of SMC alone applied to manipulate the attitude of the quadrotor, there is occurrence of an overshot and undershot. SMC, in its property, forcibly attract the actual system to the desired one. Until it is returned back to the exact position some

offset is observed resulting in the overshot and undershot from the actual trajectory. So, that, fuzzy PID controller is better for rotational roll, pitch and yaw trajectory tracking. It reduced the ISE, ITSE, and ITAE 10 times of the error obtained by using SMC. Finally, the proposed control system is better for considering any type of disturbances in the quadrotor model internally or externally and also for a good trajectory tracking performance.

5.2. Future Works

In this work the controller are designed by considering some assumptions (such as, structure quadrotor is rigid and symmetrical, the propellers are rigid, and the rotational dynamics are bounded in range to avoid singularities) in the dynamic model of quadrotor. For further investigation, obtained dynamic model and design control system without this assumptions. It might reduce unmodeled disturbance (chattering) effects.

Although, another further study could be changing the controller tuning system to particle swarm optimization (PSO) or generic algorithm (GA) instead of fuzzy tuning PID gains and design higher order SMC (HSMC), integral SMC (ISMC) instead of SMC. This might enhance its performance of tracking various trajectories.

Another possible future work is that applying the mixed controller by adding additional future on the quadrotor like sensor, camera and others equipment, and then predict future air condition and disturbance using neural network for forecasting the weather condition before the quadrotor start fly. In this case, the controller take pre-action to reject prediction disturbances.

References

[1] R. Jategaonkar, Flight vehicle system identification a time domain methodology, Reston, Virginia: American Institute of Aeronautics and Astronautics Inc, 2015.

[2] D. Norris, Build Your Own Quadcopter, New York, Chicago: McGraw-Hill Education, 2014.

[3] Vachtsevanos, Kimon P. Valavanis, George J., Handbook UAV, New York, London: Springer, 2015.

[4] Q. Quan, Introduction to Multicopter Design and Design, Beijing,china: Springer, 2017.

[5] S. Bouabdallah, A. Noth, and R. Siegwart, "PID vs LQ control techniques applied to an indoor micro quadrotor," in *in International Conference on Intelligent Robots and Systems*, 2004.

[6] P. Pounds, R. Mahony, and P. Corke, "Modelling and control of a quadrotor," in *Australasian conference on robotics and automation*, Auckland, NZ, 2006.

[7] T. Madani and A. Benallegue, "Backstepping Control for a Quadrotor Helicopter," in *IEEE/RSJ International Conference on Intelligent Robots and Systems*, 2006.

[8] S. Bouabdallah and R. Siegwart, "Backstepping and sliding-mode techniques applied to an indoor micro quadrotor," in *IEEE International Conference on Robotics and Automation*, Barcelona, Spain, 2005.

[9] R. Xu ,U. Ozguner, "Sliding mode control of a quadrotor helicopter," in *Proceedings of the 45th IEEE Conference on Decision & Control*, San Diego, CA, USA, 2006.

[10] D. Lee, H. Jin Kim, and S. Sastry, "Feedback linearization vs. adaptive sliding mode control for a quadrotor helicopter," *International Journal of Control Automation and Systems,*, vol. 3, no. 7, pp. pp. 419-428, 2009.

[11] Tengis, Ts.; Batmunkh, A., "State feedback control simulation of quadcopter model," in *IEEE 2016 11th International Forum on Strategic Technology*, Novosibirsk,Russia, 2016.

[12] A. Das, K. Subbarao, and F. Lewis, "Dynamic inversion with zero-dynamics stabilization for quadrotor control," *Control Theory & Applications, IET*, vol. 3, no. 3, p. 303–314, 2008.

[13] B. Whitehead and S. Bieniawski, "Model Reference Adaptive Control of a Quadrotor," in *AIAA Guidance, Navigation and Control Conference*, Toronto, Ontario, Canada, 2010.

[14] M.Huang, B.Xian, C.Diao, K.Yang, and Y.Feng, "Adaptive tracking control of underactuated quadrotor unmanned aerial vehicles via backstepping," in *American Control Conference*, Marriott Waterfront, Baltimore, MD, USA, 2010.

[15] W. Zeng, B. Xian, C. Diao, Q. Yin, H. Li, and Y. Yang, "Nonlinear Adaptive Regulation Control of A Quadrotor Unmanned Aerial Vehicle," in *IEEE International Conference on Control Applications*, Denver, CO, USA, 2011.

[16] D. Mellinger, Q. Lindsey, M. Shomin and V.- Kumar, "Design, Modeling, Estimation and Control for Aerial Grasping and Manipulation," in *IEEE/RSJ International Conference on Intelligent Robots and Systems*, San Francisco, CA, USA, 2011.

[17] R. Naldi, M. Furci, R.G. Sanfelice and L. Marconi, "Robust Global Trajectory Tracking for Underactuated VTOL Aerial Vehicles using Inner-Outer Loop Control Paradigms," *IEEE Transactions on Automatic Control*, vol. 62, no. 1, pp. 97 - 112, 2017.

[18] S. Bouabdallah, "Design and Control of Quadrotors with Application to Autonomous Flying," *OAI, MSc thesis Zurich*, vol. 10, no. 5775, 2007.

[19] M. De Lellis Costa de Oliveira, "Modeling, Identification and Control of a Quadrotor Aircraft," in *MSc thesis Czech Technical University in Prague Faculty of Electrical Engineering Department of Control Engineering*, Prague, June, 2011.

[20] R. Tesfaye, "Modeling and Control of a Quad-rotor Unmanned Aerial Vehicle at Hovering Position," in *Addis Ababa Institute of Technology electrical and computer engineering MSc Thesis*, Addis Ababa, Ethiopia, 2012.

[21] C. Wang, B. Song, P. Huang, C. Tang, "Trajectory Tracking Control for Quadrotor Robot Subject to Payload Variation and Wind Gust Disturbance," *J' Intell Robot Syst,* 2016.

[22] Nizar Hadi Abbas,Ahmed Ramz Sami, "Tuning of PID Controllers for Quadcopter System using Hybrid Memory based Gravitational Search Algorithm – Particle Swarm Optimization," *International Journal of Computer Applications,* vol. 172, no. 4, August 2017.

[23] Y. Bouzid, H. Siguerdidjane, Y. Bestaoui, "3D Trajectory Tracking Control of Quadrotor UAV with On-Line Disturbance Compensation," in *IEEE Conference on Control Technology and Applications*, Kohala Coast, Hawai'i, USA, August, 2017.

[24] P. Johan From, J. Tommy Gravdahl, K. Ytterstad Pettersen, Vehicle Manipulator System, Verlag, London: Springler, 2014.

[25] A. Rezoug, M. Hamerlain, Z. Achour and M. Tadjine, "Applied of an Adaptive Higher Order Sliding Mode Controller to Quadrotor Trajectory Tracking," in *IEEE International Conference on Control System, Computing and Engineering*, Penang, Malaysia, November, 2015.

[26] O. Gherouat, D. Matouk, A. Hassam and F. Abdessemed, "Modeling and Sliding Mode Control of a Quadrotor Unmanned Aerial Vehicle," *J. Automation and Systems Engineering,* vol. 10, no. 3, pp. 150-157, 2016.

[27] Abraham Villanueva, B. Castillo-Toledo and Eduardo Bayro-Corrochano, "Multi-mode Flight Sliding Mode Control System for a Quadrotor," in *2015 International Conference on Unmanned Aircraft Systems (ICUAS)*, Denver, Colorado, USA, June, 2015.

[28] Yi Kui, Gu Feng, Yang Liying, He Yuqing, Han Jianda, "Sliding Mode Control for a Quadrotor Slung Load System," in *Proceedings of the 36th Chinese Control Conference*, Dalian, China, July 26-28, 2017.

[29] S. Norouzi Ghazbi,Y. Aghli and M. Alimohammadi, "Quadrotors Unmanned Aerial Vehicles: A Review," *International Journal on Smart Sensing and Intelligent Systems,* vol. 9, no. 1, March ,2016.

[30] L. Jiukin, Sliding Mode Control Using MATLAB, beinjig, Chaina: Elsevier Inc, 2017.

[31] Jinkun Liu and Xinhua Wang, Advanced Sliding Mode Control for Mechanical Systems, Dordrecht ,London, New York: Springer, 2014.

[32] Nabil Derbel, Jawhar Ghommam and Quanmin Zhu, Applications of Sliding Mode Control, Singapore: Springer, 2017.

[33] R. Thomas, "Sliding Mode Controller for a Quadrotor," University of Victoria, India, 2017.

[34] Ceren Cömert and Coşku Kasnakoğlu, "Comparing and Developing PID and Sliding Mode Controllers for Quadrotor," *International Journal of Mechanical Engineering and Robotics Research,* vol. 6, no. 3, May 2017.

[35] M. Ahmed, Sliding Mode Control for Switched Mode Power Supplies, Lappeenranta : Lappeenranta University of Technology, December 2004.

[36] E. Abbasi, M. J. Mahjoob, R. Yazdanpanah, "Controlling of Quadrotor UAV Using a Fuzzy System for Tuning the PID Gains in Hovering Mode," in *Center for Mechatronics and Automation*, Tehran, Iran, 2013.

[37] E. Kuantama, T. Vesselenyi, S. Dzitac, R. Tarca, "PID and Fuzzy-PID Control Model for Quadcopter Attitude with Disturbance Parameter," *International Journal of Computers Communications & Control,* vol. 12, no. 4, pp. 519-532, 2017.

[38] Abdullah I. Al-Odienat, Ayman A. Al-Lawama, "The Advantages of PID Fuzzy Controllers Over the Conventional Types," *American Journal of Applied Sciences,* vol. 6, no. 5, pp. 653-658, 2008.

[39] A.Visioli, "Tuning of PID controllers with fuzzy logic," in *IEE Proceedings - Control Theory Application*, Brescia, Italy, January 2001.

Appendix A

Mathematical calculation of control performance index

$\mathrm{ISE} = \int \mathrm{e}^2(\mathrm{t})\,\mathrm{dt}$	Integral square error
$\mathrm{IAE} = \int \lvert e(t) \rvert\,\mathrm{dt}$	Integral absolute error
$\mathrm{ITSE} = \int \mathrm{te}^2(\mathrm{t})\,\mathrm{dt}$	Integral time square error
$\mathrm{ITAE} = \int \mathrm{t}\lvert e(t) \rvert\,\mathrm{dt}$	Integral time absolute error